NACA TN 3064 3365

TECH LIBRARY KAFB, NM
0066293

NATIONAL ADVISORY COMMITTEE FOR AERONAUTICS

TECHNICAL NOTE 3064

DATA ON THE COMPRESSIVE STRENGTH OF SKIN-STRINGER PANELS OF VARIOUS MATERIALS

By Norris F. Dow, William A. Hickman, and B. Walter Rosen

Langley Aeronautical Laboratory
Langley Field, Va.

Washington
January 1954

NACA LIBRARY

TECH LIBRARY KAFB, NM
0066293

B

NATIONAL ADVISORY COMMITTEE FOR AERONAUTICS

TECHNICAL NOTE 3064

DATA ON THE COMPRESSIVE STRENGTH OF SKIN-STRINGER PANELS OF VARIOUS MATERIALS

By Norris F. Dow, William A. Hickman, and B. Walter Rosen

SUMMARY

Flat skin-stringer compression panels of stainless steel, mild steel, titanium, copper, four aluminum alloys, and a magnesium alloy were tested. The results show the effect of variations in yield stress, Young's modulus, and both yield stress and Young's modulus for constant yield strain on the average stress at maximum load, on the stress for local buckling, and on the load-shortening characteristics of the panels.

INTRODUCTION

The materials from which aircraft structures are made are always subject to change as manufacturers of materials improve their products and as changing aircraft forms and requirements demand new and stronger materials for the structure. Even with a given material, during a single flight an airplane may be subjected to a range of temperature conditions that will cause the properties of the material to change appreciably.

In order to make proper allowance in design for all these changing conditions, correlation must be effected between material properties and structural strength. In compression, proper correlation requires consideration of both the stress at which buckling occurs and the average stress at maximum load. For simple shapes, the relationship between the stress-strain curve for the material and the buckling strength has been fairly thoroughly investigated (refs. 1 to 4). Again, for simple shapes, a start has been made on effecting the correlation between material properties and the average stress at maximum load (refs. 2 to 5). In the case of more complex shapes, such as the longitudinally stiffened panel with which the present paper is concerned, considerations of the effect of varying material properties have been in the main restricted to the determination of the relatively small corrections required to bring test results into line with the results to be expected when materials of guaranteed minimum properties are used. Examples of studies of such corrections are references 6 and 7. Studies of effects of large changes in material properties have been begun by Wimer (ref. 8) and by Holt (ref. 9).

In the present study, in order to provide data which may be used as a basis for analysis of the effect of variation in material properties on the compressive strengths of panels, a wide range of panel proportions and materials were experimentally investigated. The proportions were selected to correspond to those investigated in previous studies by the National Advisory Committee for Aeronautics (for example, refs. 10 to 12). The materials were selected to provide information on the effect on panel strength of the following:

Phase I: A variation in compressive yield stress with a substantially constant Young's modulus

Phase II: A variation in Young's modulus with a substantially constant compressive yield stress

Phase III: A variation in both Young's modulus and compressive yield stress

Experimental measurements were made of average stress at maximum load, stress for local buckling of the sheet, and of the relationship between average stress and unit shortening which defines, for any given unit shortening, the effectiveness of the cross section for resisting additional deformation.

SYMBOLS

c	coefficient of end fixity in Euler column formula (taken as 3.75 for all tests, as in refs. 10 and 11)
E	Young's modulus of elasticity, ksi
L/ρ	slenderness ratio
ϵ	strain
$\bar{\epsilon}$	unit shortening
$\bar{\epsilon}_f$	unit shortening at maximum load
ϵ_{cy}	compressive yield strain (0.2-percent offset)
σ	stress, ksi
$\bar{\sigma}$	average stress, ksi

$\bar{\sigma}_f$	average stress at maximum load, ksi
σ_{cr}	stress for local buckling of sheet, ksi
σ_{cy}	compressive yield stress (0.2-percent offset), ksi
b_F	width of outstanding flange of stringer, in.
b_S	stringer spacing, in.
b_W	width of web of stringer, in.
L	length of panel, in.
r_W	bend radius of stringer, in.
t_S	skin thickness, in.
t_W	stringer thickness, in.
K,n	constants used in Ramberg-Osgood representation of stress-strain curves (ref. 13)

Symbols used for the various panel dimensions are also given in figure 1.

MATERIALS INVESTIGATED

For the purpose of providing data on the effects of material properties, the specimens were selected to permit an evaluation based on the effects of compressive yield stress and Young's modulus. On this basis, the investigation covered three phases, as follows:

Phase I made use of materials selected to provide a variation in compressive yield stress with a substantially constant Young's modulus.

Phase II made use of materials selected to provide a variation in Young's modulus with a substantially constant compressive yield stress.

Phase III made use of materials selected to provide a variation in both Young's modulus and compressive yield stress with a substantially constant compressive yield strain.

The materials used in each of the three phases covered, together with their pertinent properties, are presented in the following table:

Material	E, ksi	σ_{cy}, ksi	ϵ_{cy}
Phase I			
75S-T6 aluminum alloy	10.5×10^3	72.6	0.0089
61S-T6 aluminum alloy	10.5	43.3	.0061
52S - $\frac{1}{4}$H aluminum alloy	10.2	25.6	.0045
75S-0 aluminum alloy	10.5	15.1	.0034
Phase II			
SAE 1010 mild steel	29.3×10^3	25.2	0.0029
Copper	15.7	25.6	.0036
52S - $\frac{1}{4}$H aluminum alloy	10.2	25.6	.0045
FS-1h magnesium alloy	6.5	24.6	.0058
Phase III			
18-8 - $\frac{3}{4}$H stainless steel	29.0×10^3	111.3	0.0058
Ti - $\frac{1}{4}$H titanium	14.5	68.2	.0067
61S-T6 aluminum alloy	10.5	43.3	.0061
FS-1h magnesium alloy	6.5	24.6	.0058

The average longitudinal stress-strain curves obtained from the flat-sheet materials in their final condition as used for the fabrication of the test panels are presented in figures 2(a), 2(b), and 2(c) for phases I, II, and III of the investigation, respectively. Both the steel and the copper materials required various treatments in order to give them the properties shown; accordingly, their stress-strain curves as given are not representative of commercially available products.

TEST SPECIMENS

The proportions of the panel cross sections were varied systematically from a minimum b_s/t_s of 25 and a minimum b_w/t_w of 12.5. Panel specimens were divided into two groups. In one group the cross section

was varied by increasing all width-thickness ratios for the plate elements in the same proportion. In the other group, the stiffener cross section was held constant and the stiffener spacing was varied. Nominal dimensions of the test specimens and a typical cross section are given in table 1 and figure 1, respectively.

For simplicity in identifying the specimens, they are designated by numbers indicating pertinent dimension ratios separated by dashes as follows:

First number represents the ratio b_W/t_W

Second number represents the ratio b_S/t_S

Third number represents the ratio L/ρ

Thus, panel 12.5-25-20 has a ratio b_W/t_W of 12.5, a ratio b_S/t_S of 25, and L/ρ of 20. In all cases, actual sheet thicknesses were measured before construction was started, and all dimensions were adjusted so that the completed specimens had, within 2 percent, the following dimension ratios:

Ratio of stringer thickness to skin thickness, t_W/t_S	Ratio of stringer web width to thickness, b_W/t_W	Ratio of stringer spacing to skin thickness, b_S/t_S	Ratio of specimen length to radius of gyration, L/ρ
1.00	12.5	25	20, 40
1.00	18.75	37.5	20, 40, 70
1.00	25	50	20, 40, 70, 110
1.00	37.5	75	20, 40, 70, 110
1.00	12.5	25	20, 40
1.00	12.5	37.5	20, 40, 70
1.00	12.5	50	20, 40, 70, 110
1.00	12.5	75	20, 40, 70, 110

On all specimens, stringers were attached to sheet with 1/8-inch-diameter universal-head rivets (AN470-4-5) at 3/8-inch pitch. In an effort to keep the effect of riveting on the strength of the panels consistent for all specimens, rivet materials were selected to have the same nominal stiffnesses as the materials of the panels in which they were used and, also, as nearly as feasible, the same strengths relative to the strengths of their respective panel materials. The rivet materials used are listed in table 2 together with measured values of their shear and tensile strengths.

In this investigation, as in many experimental investigations, perfect control of all material properties was not possible. Although the average longitudinal properties of the sheet before forming were, in general, held to within 5 percent of the desired values, variations from the average values were appreciable for a few materials (for example, the titanium). Moreover, the transverse properties in some cases were appreciably different from the average longitudinal properties (for example, the stainless steel), as were the longitudinal properties in the corners of the Z-stringers after forming (for example, the 75S-0 aluminum alloy). Similar difficulties were encountered with the rivets. In some cases, rivet materials could not be found which bore the desired relationships in both strength and stiffness to the properties of the material of the panels in which they were used. (For example, all rivet materials investigated of the desired stiffness for the mild steel panels were too strong. See table 2.) In general, the unavoidable deviations in rivet properties from those desired were probably small enough with the strong riveting used (see ref. 14) so that they did not influence the results of the panel tests appreciably. The effects of variation in material properties from the average, transversely (see ref. 15), or due to forming (see ref. 16) unquestionably influenced the results in some cases. The magnitude of the variations from the desired properties are indicated in table 3 by the numerical tabulations of values of moduli and yield stresses. For purposes of comparison, average properties are also given in table 4 in terms of the Ramberg-Osgood (ref. 13) analytical representation of the stress-strain curve.

METHODS OF TESTING

All specimens were compressed flat-ended, without side support. The ends of the specimens were ground accurately flat and parallel in a special grinder and the method of alinement in the testing machine was such as to insure uniform bearing on the ends of the specimen. Flat-end tests such as these have been suggested in previous investigations (for example, refs. 10 and 11) to yield a value of end-fixity coefficient c of 3.75.

The testing machine used was the 1,200-000-pound-capacity hydraulic machine of the Langley structures research laboratory. This machine was especially adapted to these panel tests by rearrangement of the loading system so that, as the upper crosshead moved downward to apply load to the specimen, it also applied load to a 300,000-pound-capacity hydraulic jack. With this arrangement (see fig. 3), as the specimen reached maximum load, continued crosshead motion was opposed and controlled by the jack so that even beyond maximum load the load-distortion characteristics of the specimen could be observed. The jack was located external to the weighing system of the testing machine so that the accuracy of weighing,

except for possible inertia effects in the unloading region beyond maximum load, of one-half of 1 percent of the load was maintained. Inertia effects were most pronounced when the load-distortion curves had the greatest negative slopes. In these regions, the exact values of load for given distortion depend upon the mass and stiffness characteristics of the adjacent load-applying structure. (See ref. 17.)

The loads for local buckling of the sheet were determined by the strain-reversal method (ref. 18) as the loads at which plots of the strains near buckle crests first showed decreasing strains with increasing loads. These plots were obtained autographically from 12 resistance-type wire strain gages arranged in a pattern on both sides of the sheet of each specimen so that at least one gage should lie near a buckle crest.

Curves of average stress plotted against unit shortening were obtained from all specimens. The unit shortening was measured in two ways: (1) as the average of the strains indicated by four, long-gage-length, resistance-type wire strain gages mounted on the quarter-points along the length of the second and fifth stiffeners at the center of gravity of the cross section, and (2) by direct measurement adjacent to the specimen of over-all shortening of the distance between testing-machine crossheads. In most cases the measurements obtained by the latter method were used because they were evidently more reliable, as indicated both by the character of the shortening curves and by the relative values of shortening from specimen to specimen. The measurements of unit shortening were probably within 5 percent of the true values, except possibly in the regions of greatest negative slopes of the curves.

RESULTS AND DISCUSSION

Experimental results.- The experimental results are presented as tabulated values of $\overline{\sigma}_f$ (average stress at maximum load), σ_{cr} (stress for local buckling of sheet), and $\overline{\epsilon}_f$ (unit shortening at maximum load) in tables 5, 6, and 7, respectively. The curves obtained for average stress against unit shortening are presented together with the average longitudinal stress-strain curves for the panel materials (labeled σ-ϵ) in figures 4, 5, and 6 for phases I, II, and III of the investigation, respectively. It will be noted in tables 5, 6, and 7 that panel specimens are presented in the two groups previously discussed. For convenience in making comparisons, the data for the first two panels in each group have therefore been repeated. For the same reason, this repetition is found in parts (a) and (e) of figures 4, 5, and 6.

Types of distortion observed.- The distortions of the panels under load varied with the varying proportions and materials from local buckling of the plate elements to column bending of the panel as a whole. No rivet failures occurred. Panel failures were accompanied by twisting of the Z-stringers for both local buckling and column bending; observation of failure, however, was inadequate to determine whether the twisting was a cause of failure or a result of other failing modes. Twisting was accentuated when over-all bending occurred (as the panel length increased) because the panels generally bowed toward the skin so that the compressive stresses in the outstanding flanges of the Z-stringers were increased at the midlength of the panel where twisting was a maximum. The bowing toward the skin, caused by the initial curvature induced in the panels by the riveting, correspondingly reduced the compressive stresses in the skin so that buckling of the skin generally was delayed as the panel length increased. Buckling of the skin was also delayed slightly by end effects for the short panels with wide stringer spacings for which the panel length was not several times the stringer spacing.

Experimental scatter.- Despite the fact that greater control was exercised over the construction of the specimens than in previous NACA panel investigations, by the preselection of materials of desired properties and by the adjustment of dimensions according to measured sheet thicknesses to give desired rather than nominal dimension ratios, some experimental scatter still occurred in the results. This scatter is manifested: (1) by the higher values of average stress at maximum load $\overline{\sigma}_f$ which were measured in some cases (notably copper) for the panels having $L/\rho = 40$ than for the corresponding panels having $L/\rho = 20$ (table 5); (2) by the various values of stress for local buckling of the sheet σ_{cr} measured for the same cross section; and (3) by the curves of average stress against unit shortening. In part at least, the experimental scatter can be attributed to initial eccentricities in the specimens; such eccentricities would probably have greater influence on the measured values of σ_{cr} than on $\overline{\sigma}_f$, and even greater influence on the detailed character of the plots of average stress against unit shortening (figs. 4, 5, and 6). The plots of average stress against unit shortening were also affected by the work hardening of the corner material which occurred during forming of the stringers. This work hardening was sufficient in some cases (notably 75S-0, see table 3) to cause the curves of average stress against unit shortening to exceed the stress-strain curves for the unformed material. Accordingly, the shortening curves given should be considered as applicable to the individual panels as tested rather than as precisely characteristic of a given cross section and material.

Observed effects of material properties.- No detailed analysis of the test results is included herein. However, some further analysis is presented in reference 19. The following gross effects of variations in material, however, are immediately evident from the test data:

For phase I (σ_{cy} varied, E constant):

(1) An increase in σ_{cy} always increased the value of $\bar{\sigma}_f$ (table 5).

(2) An increase in σ_{cy} increased the value of σ_{cr} whenever buckling occurred in the plastic stress range (table 6).

(3) An increase in σ_{cy} generally increased the value of $\bar{\epsilon}_f$ (table 7). Exceptions to this statement occurred particularly for the short panels ($L/\rho = 20$) of 75S-0 material, for which the plots of average stress against unit shortening had very flat maximums (fig. 4), probably in part because of the continuously rising stress-strain curve for this material beyond the yield. This continuously rising stress-strain curve is indicated pictorially in figure 2(a) and analytically, as noted in table 4, by the fact that the Ramberg-Osgood formulation is inadequate to describe the curve. In fact, above the yield stress a straight line with a substantially positive slope is an excellent representation of the measured stress-strain properties (this might be thought of as representative of continuously decreasing values with increasing stress of the exponent n in the Ramberg-Osgood formula).

(4) An increase in σ_{cy} (which was accompanied in general by smaller slopes of the stress-strain curves at stresses beyond the yield stress; in the Ramberg-Osgood formulation of the stress-strain curve, such smaller slopes are represented by larger values of the exponent n, see table 4) generally caused the average stress carried by the panels at values of unit shortening greater than $\bar{\epsilon}_f$ to decrease more rapidly as values of $\bar{\epsilon}$ were increased.

For phase II (E varied, σ_{cy} constant):

(1) An increase in E always increased the value of $\bar{\sigma}_f$ (table 5).

(2) An increase in E generally increased the value of σ_{cr} (table 6). The one exception to this statement occurred for the cross section with the smallest ratios of width to thickness of its plate elements ($b_S/t_S = 25$); for this section the buckling stresses were well up in the plastic range ($\sigma_{cr} = 21.8$ ksi for 52S-$\frac{1}{4}$H aluminum alloy, $\sigma_{cr} = 22.7$ ksi for FS-1h magnesium alloy, see table 6).

(3) An increase in E generally tended to decrease the value of $\bar{\epsilon}_f$ (table 7). Although there were numerous individual exceptions to this statement, the trend is in the direction of somewhat smaller values of

unit shortening at failure for higher values of the modulus, with the exception of short panels having small values of width-thickness ratios for their plate elements. For these latter groups of panels (for which failure was primarily by local buckling), the values of $\bar{\epsilon}_f$ tended to increase with increasing values of E. The fact that increases in E did not produce more substantial decreases in $\bar{\epsilon}_f$ may be associated with the more continuously rising stress-strain curves at high stresses for the SAE 1010 and the copper materials than for the 52S - $\frac{1}{4}$H and the FS-1h (see fig. 2(b)). The sharper knees of the curves for the latter two materials are also indicated by the higher values of n in their Ramberg-Osgood formulation (see table 4).

(4) An increase in E appeared to cause the average stress carried by the panels at values of unit shortening greater than $\bar{\epsilon}_f$ to decrease somewhat less rapidly as $\bar{\epsilon}$ increased (fig. 5). This trend, however, may be more associated with the more continuously rising stress-strain curves at high stresses of the stiffer materials than with their higher modulus values (see discussion of effect of variation of $\bar{\epsilon}_f$ with E).

For phase III (E and σ_{cy} varied, ϵ_{cy} constant):

(1) An increase in both E and σ_{cy} always increased the value of $\bar{\sigma}_f$ (table 5).

(2) An increase in both E and σ_{cy} always increased the value of σ_{cr} (table 6).

(3) An increase in both E and σ_{cy} tended to increase the value of $\bar{\epsilon}_f$ (table 7) for the shortest panels ($L/\rho = 20$) for which failure was primarily by local buckling. For the longest panels ($L/\rho = 110$), for which failure was primarily by column bending, the value of $\bar{\epsilon}_f$ was fairly constant despite the variations in E and σ_{cy}. The increasing values of $\bar{\epsilon}_f$ with increasing E and σ_{cy} in this phase of the investigation may also be attributed to the more continuously rising stress-strain curves of the 18-8 - $\frac{3}{4}$H and the Ti - $\frac{1}{4}$H (see fig. 2(c)). The values of n in the Ramberg-Osgood formulation for these two materials (see table 4) are the smallest of those for all the materials investigated. The titanium panels consistently gave the highest values of $\bar{\epsilon}_f$, particularly in the shorter lengths. The particularly high values of $\bar{\epsilon}_f$

for the titanium may be in part associated with the fact that this material did not show increased values of σ_{cy} in the corners of the Z-stringers after forming (table 3); the associated unit-shortening curves (fig. 6) were gently rounded, without sharp knees, and with fairly flat maximums.

(4) An increase in both E and σ_{cy} had no appreciable effect upon the relative rate of decrease of load-carrying capacity of the panels with increasing values of unit shortening for values of $\bar{\epsilon}$ greater than $\bar{\epsilon}_f$.

CONCLUDING REMARKS

In order to provide data to be used as a basis for the correlation of the strength of skin-stringer compression panels with their material stress-strain properties, tests were made of panels of a wide range of systematically varied proportions and materials. The gross effects of variations in yield stress, Young's modulus, and both yield stress and Young's modulus for constant yield strain are revealed by the data obtained on the average stress at maximum load and on the stress for local buckling. The measured curves of average stress against unit shortening presented, however, provide more complete detailed information on the characteristics of each cross section of each material to use as a basis for analysis.

Langley Aeronautical Laboratory,
National Advisory Committee for Aeronautics,
Langley Field, Va., November 13, 1953.

REFERENCES

1. Stowell, Elbridge Z.: A Unified Theory of Plastic Buckling of Columns and Plates. NACA Rep. 898, 1948. (Supersedes NACA TN 1556.)

2. Duberg, John E., and Wilder, Thomas W., III: Inelastic Column Behavior. NACA Rep. 1072, 1952. (Supersedes NACA TN 2267.)

3. Onat, E. T., and Drucker, D. C.: Inelastic Instability and Incremental Theories of Plasticity. Jour. Aero. Sci., vol. 20, no. 3, Mar. 1953, pp. 181-186.

4. Stowell, Elbridge Z., Heimerl, George J., Libove, Charles, and Lundquist, Eugene E.: Buckling Stresses for Flat Plates and Sections. Proc. Am. Soc. Civil Eng., vol. 77, separate no. 77, July 1951, pp. 1-31.

5. Stowell, Elbridge Z.: Compressive Strength of Flanges. NACA Rep. 1029, 1951. (Supersedes NACA TN 2020.)

6. Heimerl, George J.: Methods of Constructing Charts for Adjusting Test Results for the Compressive Strength of Plates for Differences in Material Properties. NACA TN 1564, 1948.

7. Hoskin, B. C., and Joyce, N. B.: Correction of Compressive Test Results on Some Aluminum and Magnesium Alloys for Material Properties. SM Note 199, Aero. Res. Labs. (Melbourne), July 1952.

8. Wimer, H. Dudley, Jr.: Stability of Thin-Walled Compression Members. Proc. Am. Soc. Civil Eng., vol. 74, no. 5, May 1948, pp. 655-668.

9. Holt, Marshall: Results of Edge-Compression Tests on Stiffened Flat-Sheet Panels of Alclad and Nonclad 14S-T6, 24S-T3, and 75S-T6 Aluminum Alloys. NACA TN 3023, 1954.

10. Dow, Norris F., Hickman, William A., and McCracken, Howard L.: Compressive-Strength Comparisons of Panels Having Aluminum-Alloy Sheet and Stiffeners With Panels Having Magnesium-Alloy Sheet and Aluminum-Alloy Stiffeners. NACA TN 1274, 1947.

11. Dow, Norris F., and Hickman, William A.: Comparison of the Structural Efficiency of Panels Having Straight-Web and Curved-Web Y-Section Stiffeners. NACA TN 1787, 1949.

12. Hickman, William A., and Dow, Norris F.: Direct-Reading Design Charts for 24S-T3 Aluminum-Alloy Flat Compression Panels Having Longitudinal Formed Hat-Section Stiffeners and Comparisons With Panels Having Z-Section Stiffeners. NACA TN 2792, 1953.

13. Ramberg, Walter, and Osgood, William R.: Description of Stress-Strain Curves by Three Parameters. NACA TN 902, 1943.

14. Dow, Norris F., Hickman, William A., and Rosen, B. Walter: Effect of Variation in Rivet Strength on the Average Stress at Maximum Load for Aluminum-Alloy, Flat, Z-Stiffened Compression Panels That Fail by Local Buckling. NACA TN 2963, 1953.

15. Watter, Michael, and Lincoln, Rush A.: Strength of Stainless Steel Structural Members as Function of Design. First ed., Allegheny Ludlum Steel Corp. (Pittsburgh), 1950.

16. Woods, Walter, and Heimerl, George J.: Effect of Brake Forming in Various Tempers on the Strength of Alclad 75S-T Aluminum-Alloy Sheet. NACA TN 1162, 1947.

17. Freudenthal, Alfred M.: The Inelastic Behavior of Engineering Materials and Structures. John Wiley & Sons, Inc., 1950, pp. 527-534.

18. Hu, Pai C., Lundquist, Eugene E., and Batdorf, S. B.: Effect of Small Deviations From Flatness on Effective Width and Buckling of Plates in Compression. NACA TN 1124, 1946.

19. Dow, Norris F., and Anderson, Roger A.: Prediction of Ultimate Strength of Skin-Stringer Panels From Load-Shortening Curves. Presented at Annual Meeting of Inst. Aero. Sci., Jan. 1954.

TABLE 1

NOMINAL DIMENSIONS OF TEST SPECIMENS

[Symbols used for panel dimensions are given in fig. 1]

Panel number (a)	t_s, in.	t_w, in.	b_s, in.	b_w, in.	L, in.
12.5-25-20	0.064	0.064	1.60	0.80	6.32
12.5-25-40	.064	.064	1.60	.80	12.64
18.75-37.5-20	.064	.064	2.40	1.20	9.40
18.75-37.5-40	.064	.064	2.40	1.20	18.80
18.75-37.5-70	.064	.064	2.40	1.20	32.90
25-50-20	.064	.064	3.20	1.60	12.40
25-50-40	.064	.064	3.20	1.60	24.80
25-50-70	.064	.064	3.20	1.60	43.40
25-50-110	.064	.064	3.20	1.60	68.20
37.5-75-20	.064	.064	4.80	2.40	18.12
37.5-75-40	.064	.064	4.80	2.40	36.24
37.5-75-70	.064	.064	4.80	2.40	63.42
37.5-75-110	.064	.064	4.80	2.40	99.66
12.5-37.5-20	.064	.064	2.40	.80	5.92
12.5-37.5-40	.064	.064	2.40	.80	11.84
12.5-37.5-70	.064	.064	2.40	.80	20.72
12.5-50-20	.064	.064	3.20	.80	5.56
12.5-50-40	.064	.064	3.20	.80	11.12
12.5-50-70	.064	.064	3.20	.80	19.46
12.5-50-110	.064	.064	3.20	.80	30.58
12.5-75-20	.064	.064	4.80	.80	5.02
12.5-75-40	.064	.064	4.80	.80	10.04
12.5-75-70	.064	.064	4.80	.80	17.57
12.5-75-110	.064	.064	4.80	.80	27.61

[a]First number gives value of b_w/t_w, second number gives value of b_s/t_s, and third number gives value of L/ρ.

TABLE 2

PROPERTIES OF RIVET MATERIALS USED IN TEST SPECIMENS

Panel material	Rivet material	Rivet ultimate shear stress, ksi	Rivet ultimate tensile stress, ksi
18-8 - $\frac{3}{4}$H	Monel	66.2	118.4
SAE 1010	[a]Iron	28.5	45.7
Ti - $\frac{1}{4}$H	Beryllium-Copper	58.0	89.5
Copper	[a]Copper	18.0	41.8
75S-T6	24S-T4	47.9	57.3
61S-T6	53S-T61	26.5	38.9
52S - $\frac{1}{4}$H	53S-T4	24.1	33.2
75S-0	2SF	13.2	17.2
FS-1h	FS-1	22.4	34.0

[a]In order to reduce both shear and tensile strengths without appreciably reducing the tensile stiffnesses, both iron and copper rivets were notched with a thin circumferential cut at the parting line of the two sheets. These notches were essentially closed after driving. Stresses given are based on the full shank area.

TABLE 3

MEASURED VALUES OF YOUNG'S MODULUS AND COMPRESSIVE YIELD STRESS FOR MATERIALS USED FOR TEST SPECIMENS

[All values in ksi]

Material	Longitudinal						Transverse		Longitudinal in formed corners
	Maximum		Average		Minimum		Average		Average
	E	σ_{cy}	E	σ_{cy}	E	σ_{cy}	E	σ_{cy}	σ_{cy}
18-8 - $\frac{3}{4}$H	30.0×10^3	117.7	29.0×10^3	111.3	28.5×10^3	110.7	30.9×10^3	170.0	166.0
SAE 1010	33.1	26.9	29.3	25.2	24.9	24.1	31.0	30.7	46.3
Ti - $\frac{1}{4}$H	15.3	90.8	14.5	68.2	14.0	57.0	15.1	88.8	68.2
Copper	16.9	29.4	15.7	25.6	14.5	21.5	17.4	31.0	37.4
75S-T6	10.6	73.0	10.5	72.6	10.5	72.4	10.5	77.2	85.6
61S-T6	10.6	43.7	10.5	43.3	10.5	42.9	10.5	44.6	46.7
52S - $\frac{1}{4}$H	10.5	25.8	10.2	25.6	10.0	25.4	10.2	26.5	28.2
75S-0	11.0	15.5	10.5	15.1	10.1	14.7	10.6	14.8	27.5
FS-1h	6.6	25.2	6.5	24.6	6.2	23.6	6.6	25.3	31.3

TABLE 4

VALUES OF CONSTANTS FOR RAMBERG-OSGOOD FORMULATION $\epsilon = \frac{\sigma}{E} + K\left(\frac{\sigma}{E}\right)^n$

OF STRESS-STRAIN PROPERTIES OF MATERIALS USED

Material	Constants for average longitudinal stress-strain curve		Constants for average transverse stress-strain curve		Constants for average longitudinal stress-strain curve for formed corner material	
	K	n	K	n	K	n
18-8-$\frac{3}{4}$H	1.0×10^6	3.6	7.2×10^7	5.1	9.0×10^5	3.8
SAE 1010	[a]8.9×10^{13}	[a]5.8	[a]1.1×10^{21}	[a]8.0	[a]2.3×10^{11}	[a]5.0
T1-$\frac{1}{4}$H	1.6×10^9	5.1	2.2×10^{14}	9.9	1.6×10^9	5.1
Copper	2.7×10^{12}	5.4	[a]7.8×10^{21}	[a]9.0	2.7×10^{29}	12.0
75S-T6	1.8×10^{25}	14.8	8.1×10^{39}	20	2.0×10^{45}	23
61S-T6	5.2×10^{50}	22	7.2×10^{59}	31	1.3×10^{16}	8.0
52S-$\frac{1}{4}$H	8.0×10^{24}	10.6	3.2×10^{33}	14.0	2.2×10^{20}	9.0
75S-0	[a]2.1×10^{18}	[a]7.4	[a]1.5×10^{18}	[a]7.3	1.4×10^{23}	10.0
FS-1h	[b]7.8×10^{39}	[b]18	[b]2.6×10^{150}	[b]65	3.3×10^{13}	7.0

[a]Ramberg-Osgood formula gives good representation of the stress-strain curve for stresses less than or approximately equal to the yield stress. For higher stresses the following equations may be used:

SAE 1010

(longitudinal) $\epsilon = \frac{\sigma}{E} + \left(8.9 \times 10^{13}\right)\left(\frac{\sigma}{E}\right)^{5.8} + \left(3.4 \times 10^{71}\right)\left(\frac{\sigma}{E}\right)^{24}$

(transverse) $\epsilon = \frac{\sigma}{E} + \left(1.1 \times 10^{21}\right)\left(\frac{\sigma}{E}\right)^{8.0} + \left(1.2 \times 10^{96}\right)\left(\frac{\sigma}{E}\right)^{33}$

(corner) $\epsilon = \frac{\sigma}{E} + \left(2.3 \times 10^{11}\right)\left(\frac{\sigma}{E}\right)^{5.0} + \left(1.8 \times 10^{105}\right)\left(\frac{\sigma}{E}\right)^{60}$

Copper (transverse) $\epsilon = \frac{\sigma}{E} + \left(7.8 \times 10^{21}\right)\left(\frac{\sigma}{E}\right)^{9.0} + \left(1.7 \times 10^{140}\right)\left(\frac{\sigma}{E}\right)^{52}$

75S-0

(longitudinal) $\epsilon = \left(1.08 \times 10^{-3}\right)(\sigma - 15.1) + 0.00345$

(transverse) $\epsilon = \left(1.35 \times 10^{-3}\right)(\sigma - 16.0) + 0.00472$

[b]Variation of Ramberg-Osgood formula $\left(\epsilon = \frac{\sigma}{E'} + K\left(\frac{\sigma}{E'}\right)^n - 0.0002\right)$ where $E' = 5.72 \times 10^3$ ksi gives good representation of the stress-strain curve for $\sigma \geq 10.0$ ksi; for lower stresses, $\epsilon = \frac{\sigma}{E}$.

TABLE 5

VALUES OF AVERAGE STRESS AT MAXIMUM LOAD FOR PANELS OF VARIOUS MATERIALS

	$\bar{\sigma}_f$, ksi											
Material	75S-T6	61S-T6	52S-$\frac{1}{4}$H	75S-O	SAE 1010	Copper	52S-$\frac{1}{4}$H	F8-1h	18-8-$\frac{3}{4}$H	Ti-$\frac{1}{4}$H	61S-T6	F8-1h
E, ksi	10.5×10^3	10.3×10^3	10.2×10^3	10.5×10^3	29.3×10^3	15.7×10^3	10.2×10^3	6.5×10^3	29.0×10^3	14.5×10^3	10.3×10^3	6.5×10^3
σ_{cy}, ksi	72.6	43.3	25.6	15.1	25.2	25.6	25.6	24.6	111.3	68.2	43.3	24.6
Panel number (a)	Phase I				Phase II				Phase III			
12.5-25-20	60.4	40.0	25.8	20.9	35.9	30.1	25.8	23.1	116.2	73.3	40.0	23.1
12.5-25-40	59.8	40.1	25.2	19.7	32.9	28.1	25.2	23.4	113.0	65.4	40.1	23.4
18.75-37.5-20	50.8	33.3	22.1	17.0	32.6	27.4	22.1	19.7	93.1	64.5	33.3	19.7
18.75-37.5-40	49.0	34.2	22.5	17.0	31.7	27.4	22.5	20.1	89.3	59.2	34.2	20.1
18.75-37.5-70	40.3	33.1	21.9	15.4	28.8	26.3	21.9	19.7	77.9	43.7	33.1	19.7
25-50-20	42.2	30.6	19.5	14.4	29.2	23.6	19.5	18.0	84.1	47.5	30.6	18.0
25-50-40	41.2	30.2	19.1	14.0	30.0	25.0	19.1	17.8	77.1	44.0	30.2	17.8
25-50-70	36.5	28.3	18.8	13.8	28.8	23.5	18.8	16.6	68.9	39.1	28.3	16.6
25-50-110	24.6	21.8	18.1	12.3	----	22.3	18.1	13.5	52.1	32.0	21.8	13.5
37.5-75-20	29.8	23.2	16.5	11.6	22.8	19.2	16.5	14.0	58.2	37.5	23.2	14.0
37.5-75-40	28.7	21.7	16.3	11.4	24.0	18.8	16.3	13.2	57.0	36.6	21.7	13.2
37.5-75-70	25.1	21.5	15.8	10.9	22.9	19.1	15.8	12.6	54.2	33.7	21.5	12.6
37.5-75-110	21.0	19.0	15.0	10.2	----	16.8	15.0	11.5	43.2	----	19.0	11.5
12.5-25-20	60.4	40.0	25.8	20.9	35.9	30.1	25.8	23.1	116.2	73.3	40.0	23.1
12.5-25-40	59.8	40.1	25.2	19.7	32.9	28.1	25.2	23.4	113.0	65.4	40.1	23.4
12.5-37.5-20	50.1	33.9	21.9	17.5	34.0	27.7	21.9	20.2	94.0	56.8	33.9	20.2
12.5-37.5-40	49.7	32.8	22.1	17.0	32.1	30.4	22.1	19.8	89.8	55.2	32.8	19.8
12.5-37.5-70	39.6	32.9	21.4	15.9	30.3	25.1	21.4	19.3	86.8	46.6	32.9	19.3
12.5-50-20	45.9	30.1	19.2	14.9	29.9	24.1	19.2	18.1	92.0	49.6	30.1	18.1
12.5-50-40	42.9	29.0	18.0	14.0	30.9	25.4	18.0	17.4	82.7	45.3	29.0	17.4
12.5-50-70	33.4	27.5	18.5	13.8	29.1	23.2	18.5	16.3	68.0	37.5	27.5	16.3
12.5-50-110	21.0	19.7	16.7	12.1	25.6	20.4	16.7	12.1	55.1	29.2	19.7	12.1
12.5-75-20	37.4	25.5	16.6	12.8	23.8	20.1	16.6	15.5	69.7	48.3	25.5	15.5
12.5-75-40	34.1	23.5	15.3	11.4	23.7	18.7	15.3	13.7	60.4	43.6	23.5	13.7
12.5-75-70	27.0	21.7	14.9	11.0	22.2	18.7	14.9	12.8	50.7	30.6	21.7	12.8
12.5-75-110	16.7	15.8	13.8	10.4	22.0	16.5	13.8	10.0	39.3	14.4	15.8	10.0

[a]First number gives value of b_H/t_H, second number gives value of b_S/t_S, and third number gives value of L/ρ.

TABLE 6

VALUES OF CRITICAL STRESS FOR PANELS OF VARIOUS MATERIALS

	σ_{cr}, ksi											
Material	75S-T6	61S-T6	52S-$\frac{1}{4}$H	75S-0	SAE 1010	Copper	52S-$\frac{1}{4}$H	FS-1h	18-8-$\frac{3}{4}$H	Ti-$\frac{1}{4}$H	61S-T6	FS-1h
E, ksi	10.5×10^3	10.5×10^3	10.2×10^3	10.5×10^3	29.3×10^3	15.7×10^3	10.2×10^3	6.3×10^3	29.0×10^3	14.5×10^3	10.5×10^3	6.5×10^3
σ_{cy}, ksi	72.6	43.3	25.6	15.1	25.2	25.6	25.6	24.6	111.3	68.2	43.3	24.6
Panel number (a)	Phase I				Phase II				Phase III			
12.5-25-20	58.2	39.9	25.1	----	----	28.2	25.1	22.5	114.7	72.7	39.9	22.5
12.5-25-40	58.4	----	21.8	----	----	27.1	21.8	22.7	113.0	----	----	22.7
18.75-37.5-20	34.5	27.1	21.5	14.8	----	26.0	21.5	17.3	64.5	62.4	27.1	17.3
18.75-37.5-40	38.3	32.6	22.2	----	----	26.8	22.2	19.7	71.0	57.3	32.6	19.7
18.75-37.5-70	36.0	----	21.9	15.5	----	26.3	21.9	19.2	76.6	----	----	19.2
25-50-20	18.3	19.0	16.1	12.6	----	22.3	16.1	11.7	47.9	29.6	19.0	11.7
25-50-40	20.3	20.1	17.8	11.9	----	24.3	17.8	12.4	48.3	29.6	20.1	12.4
25-50-70	21.8	20.9	18.1	12.9	----	22.5	18.1	11.8	47.0	30.3	20.9	11.8
25-50-110	22.6	21.0	17.9	12.3	----	22.2	17.9	11.9	49.3	30.9	21.0	11.9
37.5-75-20	8.5	9.1	6.0	8.5	20.2	12.9	6.0	5.1	21.2	15.0	9.1	5.1
37.5-75-40	9.9	8.9	9.1	9.1	21.7	14.0	9.1	5.2	21.5	15.1	8.9	5.2
37.5-75-70	8.8	9.7	9.1	8.3	21.0	14.1	9.1	4.9	21.5	15.9	9.7	4.9
37.5-75-110	9.8	9.8	9.5	9.4	----	13.6	9.5	5.3	20.8	----	9.8	5.3
12.5-25-20	58.2	39.9	25.1	----	----	28.2	25.1	22.5	114.7	72.7	39.9	22.5
12.5-25-40	58.4	----	21.8	----	----	27.1	21.8	22.7	113.0	----	----	22.7
12.5-37.5-20	33.1	29.2	19.9	15.9	----	----	19.9	18.5	72.2	43.5	29.2	18.5
12.5-37.5-40	33.2	31.2	20.3	16.6	----	29.5	20.3	17.9	69.1	46.0	31.2	17.9
12.5-37.5-70	34.9	----	21.3	15.3	----	----	21.3	18.5	77.3	45.1	----	18.5
12.5-50-20	17.0	17.6	16.7	10.4	28.9	20.6	16.7	11.6	42.4	22.6	17.6	11.6
12.5-50-40	18.2	18.0	16.1	11.8	----	22.9	16.1	10.7	42.0	19.9	18.0	10.7
12.5-50-70	20.1	20.7	17.1	12.5	----	22.8	17.1	11.1	42.6	----	20.7	11.1
12.5-50-110	20.1	19.4	16.6	12.1	----	20.2	16.6	11.9	----	----	19.4	11.9
12.5-75-20	9.8	8.7	9.0	7.8	18.5	13.8	9.0	6.6	24.4	----	8.7	6.6
12.5-75-40	7.0	9.3	7.7	8.5	20.8	14.1	7.7	4.8	----	13.7	9.3	4.8
12.5-75-70	8.1	9.2	8.5	7.5	----	13.1	8.5	4.9	21.7	14.1	9.2	4.9
12.5-75-110	8.8	8.3	8.4	7.7	----	13.6	8.4	4.9	19.5	13.2	8.3	4.9

[a]First number gives value of b_w/t_w, second number gives value of b_g/t_g, and third number gives value of L/ρ.

TABLE 7

VALUES OF UNIT SHORTENING AT MAXIMUM LOAD FOR PANELS OF VARIOUS MATERIALS

	$\bar{\epsilon}_f$											
Material	75S-T6	61S-T6	52S-$\frac{1}{4}$H	75S-O	SAE 1010	Copper	52S-$\frac{1}{4}$H	FS-1h	18-8-$\frac{3}{4}$H	Ti-$\frac{1}{4}$H	61S-T6	FS-1h
E, ksi	10.5×10^3	10.5×10^3	10.2×10^3	10.5×10^3	29.5×10^3	15.7×10^3	10.2×10^3	6.5×10^3	29.0×10^3	14.5×10^3	10.5×10^3	6.5×10^3
σ_{cy}, ksi	72.6	43.3	25.6	15.1	25.2	25.6	25.6	24.6	111.3	68.2	43.3	24.6
Panel number (a)	Phase I				Phase II				Phase III			
12.5-25-20	0.0063	0.0048	0.0046	0.0065	0.0085	0.0049	0.0046	0.0046	0.0056	0.0077	0.0048	0.0046
12.5-25-40	.0063	.0047	.0040	.0055	.0028	.0046	.0040	.0044	.0057	.0067	.0047	.0044
18.75-37.5-20	.0062	.0043	.0027	.0038	.0039	.0031	.0027	.0037	.0055	-------	.0043	.0037
18.75-37.5-40	.0065	.0038	.0030	.0038	.0033	.0039	.0030	.0035	.0053	.0056	.0038	.0035
18.75-37.5-70	.0040	.0035	.0027	.0030	.0022	.0027	.0027	.0035	.0032	.0036	.0035	.0033
25-50-20	.0048	.0039	.0030	.0031	.0025	.0027	.0030	.0038	.0055	.0064	.0039	.0038
25-50-40	.0051	.0040	.0024	.0025	.0028	.0026	.0024	.0037	.0050	.0056	.0040	.0037
25-50-70	.0044	.0034	.0022	.0021	.0023	.0026	.0022	.0034	.0036	.0035	.0034	.0034
25-50-110	.0025	.0023	.0019	.0014	-------	.0020	.0019	.0024	.0023	.0024	.0023	.0024
37.5-75-20	.0046	.0035	.0030	.0026	.0025	.0023	.0030	.0029	-------	.0043	.0035	.0029
37.5-75-40	.0043	-------	.0023	.0020	.0018	.0027	.0023	.0028	.0034	.0044	-------	.0028
37.5-75-70	.0031	.0028	.0022	.0016	.0018	.0024	.0022	.0028	.0033	-------	.0028	.0028
37.5-75-110	.0026	.0022	.0019	.0012	-------	.0016	.0019	.0022	.0022	-------	.0022	.0022
12.5-25-20	.0063	.0048	.0046	.0065	.0085	.0049	.0046	.0046	.0056	.0077	.0048	.0046
12.5-25-40	.0063	.0047	.0040	.0055	.0028	.0046	.0040	.0044	.0057	.0067	.0047	.0044
12.5-37.5-20	.0070	.0043	.0029	.0037	.0028	.0033	.0029	.0041	.0037	.0066	.0043	.0041
12.5-37.5-40	.0067	.0036	.0028	.0034	.0027	.0032	.0028	.0037	.0033	.0065	.0036	.0037
12.5-37.5-70	.0043	.0033	.0025	.0025	.0025	.0028	.0025	.0034	.0040	.0042	.0033	.0034
12.5-50-20	.0075	.0047	.0032	.0038	.0018	.0025	.0032	.0043	.0077	.0074	.0047	.0043
12.5-50-40	.0064	.0045	.0026	.0040	.0018	.0030	.0026	.0040	.0055	.0044	.0045	.0040
12.5-50-70	.0038	.0035	.0024	.0016	.0024	.0023	.0024	.0033	.0037	.0039	.0035	.0033
12.5-50-110	-------	-------	.0017	.0014	.0014	.0019	.0017	.0021	.0013	.0022	-------	.0021
12.5-75-20	.0067	.0034	.0032	.0033	.0022	.0034	.0032	.0036	.0043	.0064	.0034	.0036
12.5-75-40	.0050	.0037	.0030	.0033	.0015	.0029	.0030	.0035	.0043	.0066	.0037	.0035
12.5-75-70	.0030	.0037	.0027	.0027	.0014	.0027	.0027	.0027	.0031	.0029	.0037	.0027
12.5-75-110	.0021	-------	.0020	.0019	.0022	.0017	.0020	.0022	.0020	.0011	-------	.0022

[a]First number gives value of b_W/t_W, second number gives value of b_S/t_S, and third number gives value of L/ρ.

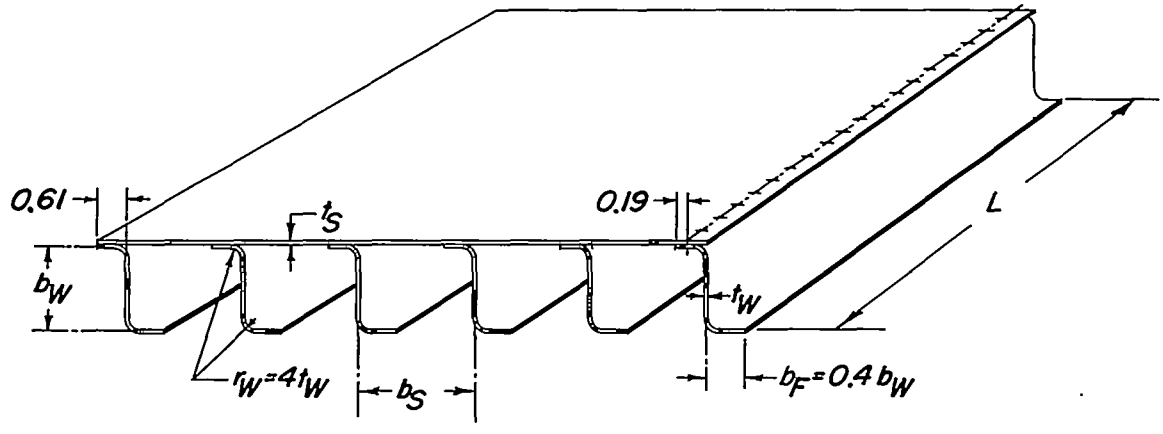

Figure 1.– Symbols for panel dimensions.

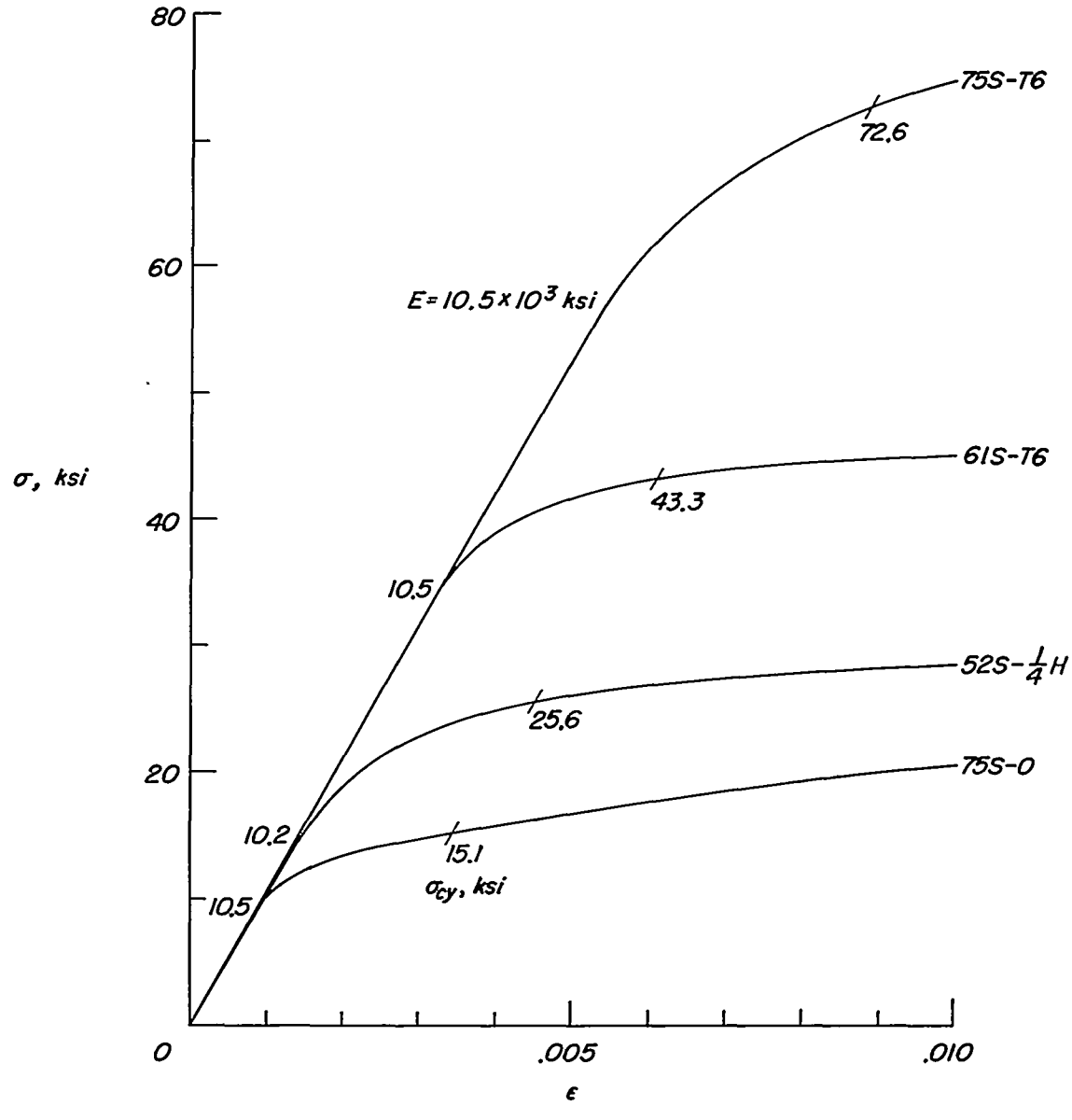

(a) σ_{cy} varied, E constant.

Figure 2.— Properties of materials used for test specimens.

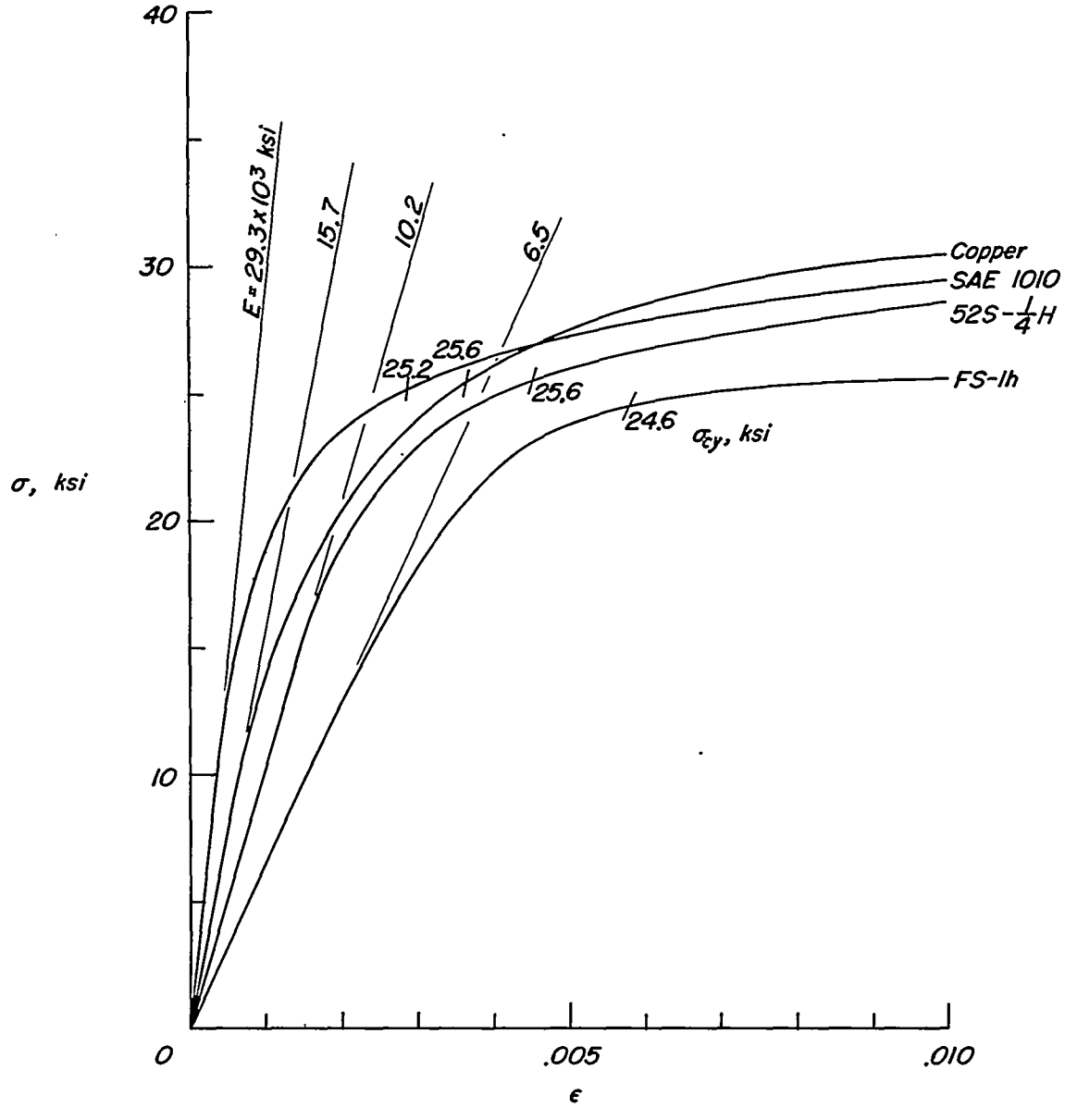

(b) E varied, σ_{cy} constant.

Figure 2.- Continued.

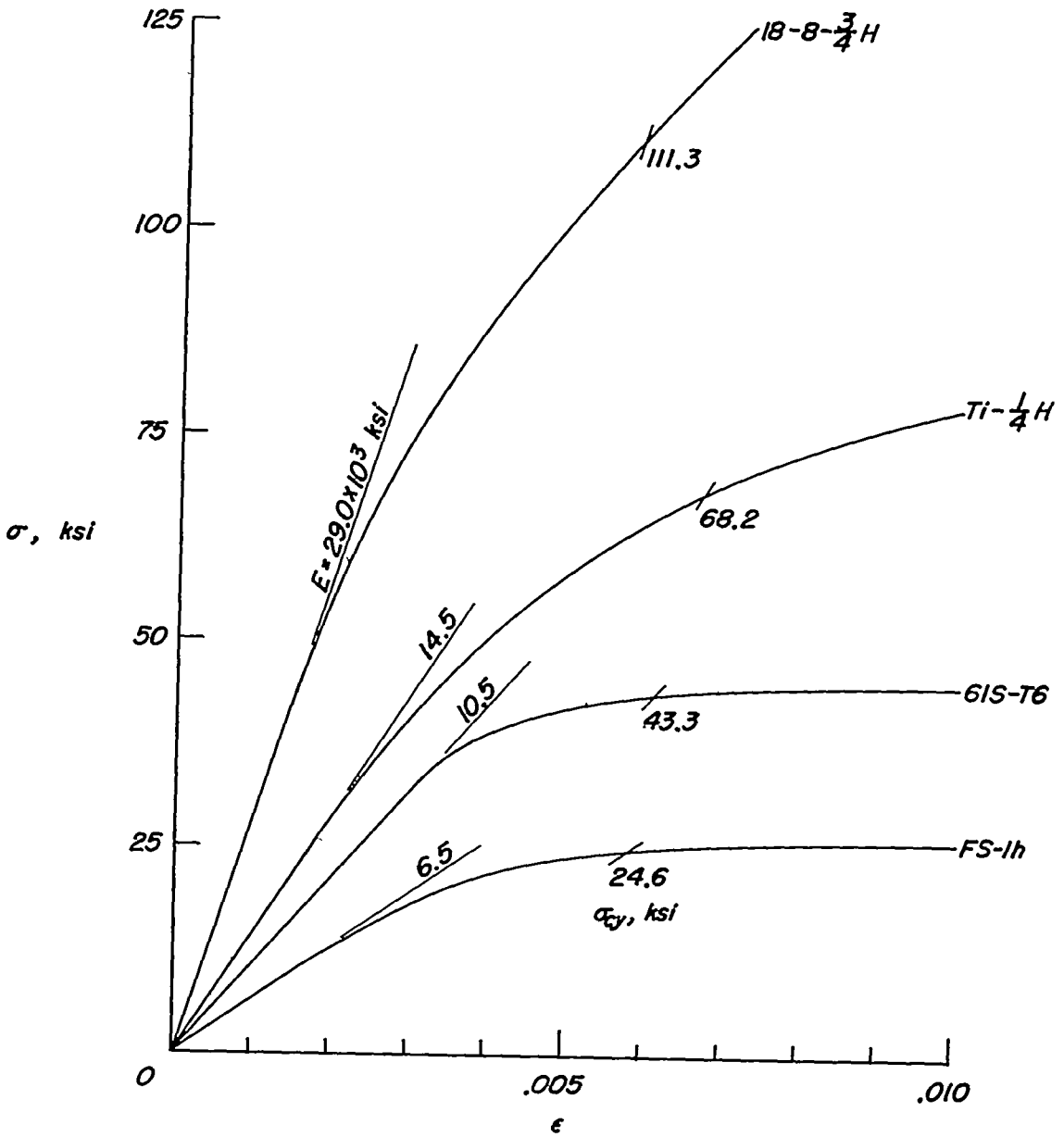

(c) E and σ_{cy} varied, ϵ_{cy} constant.

Figure 2.- Concluded.

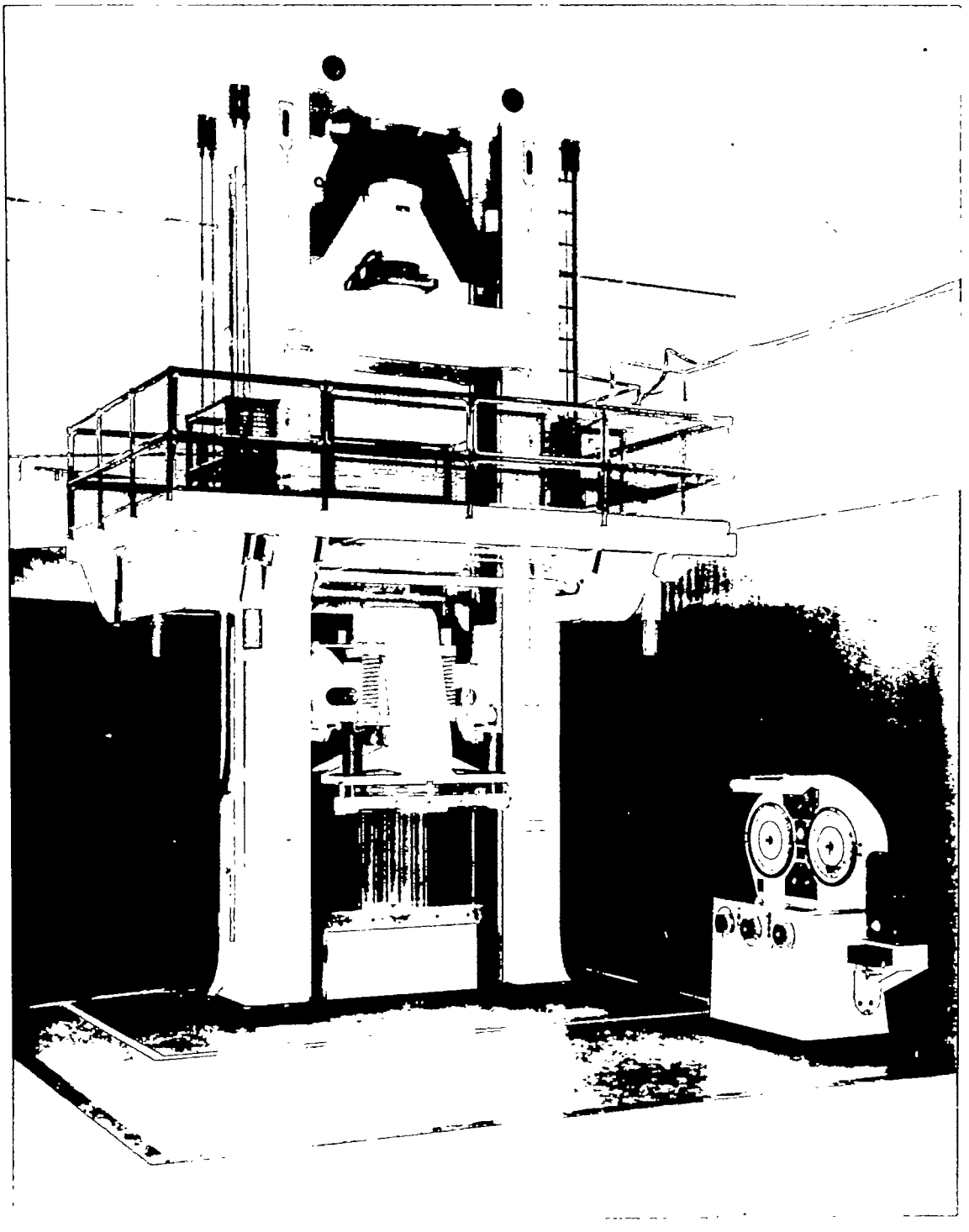

L-74492

Figure 3.- Test set-up, showing jack and yoke arrangement at top of loading system to control crosshead motion beyond maximum load.

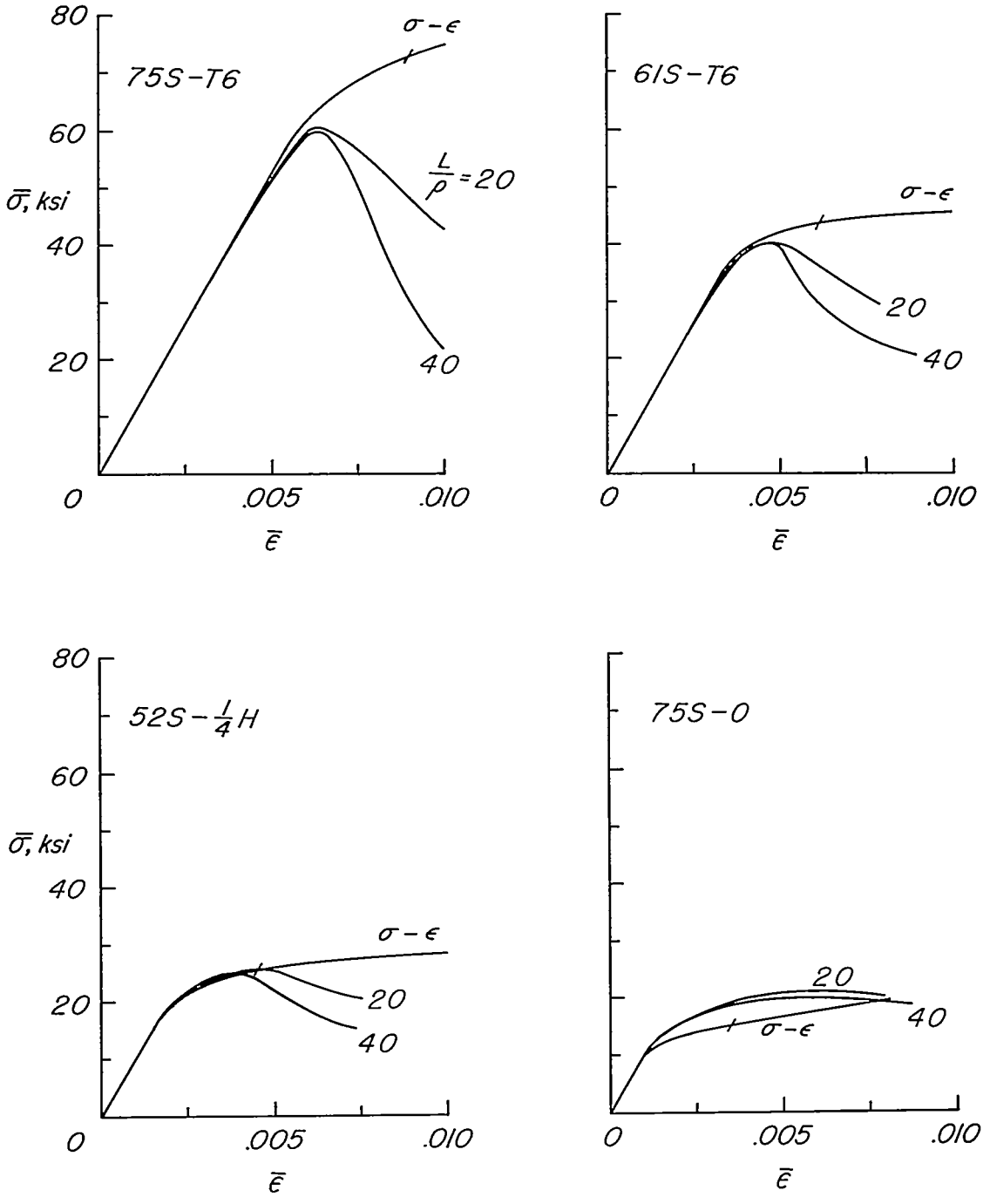

(a) $\frac{t_w}{t_s} = 1.00$; $\frac{b_w}{t_w} = 12.5$; $\frac{b_s}{t_s} = 25.$

Figure 4. — Curves of average stress against unit shortening for phase I panels.

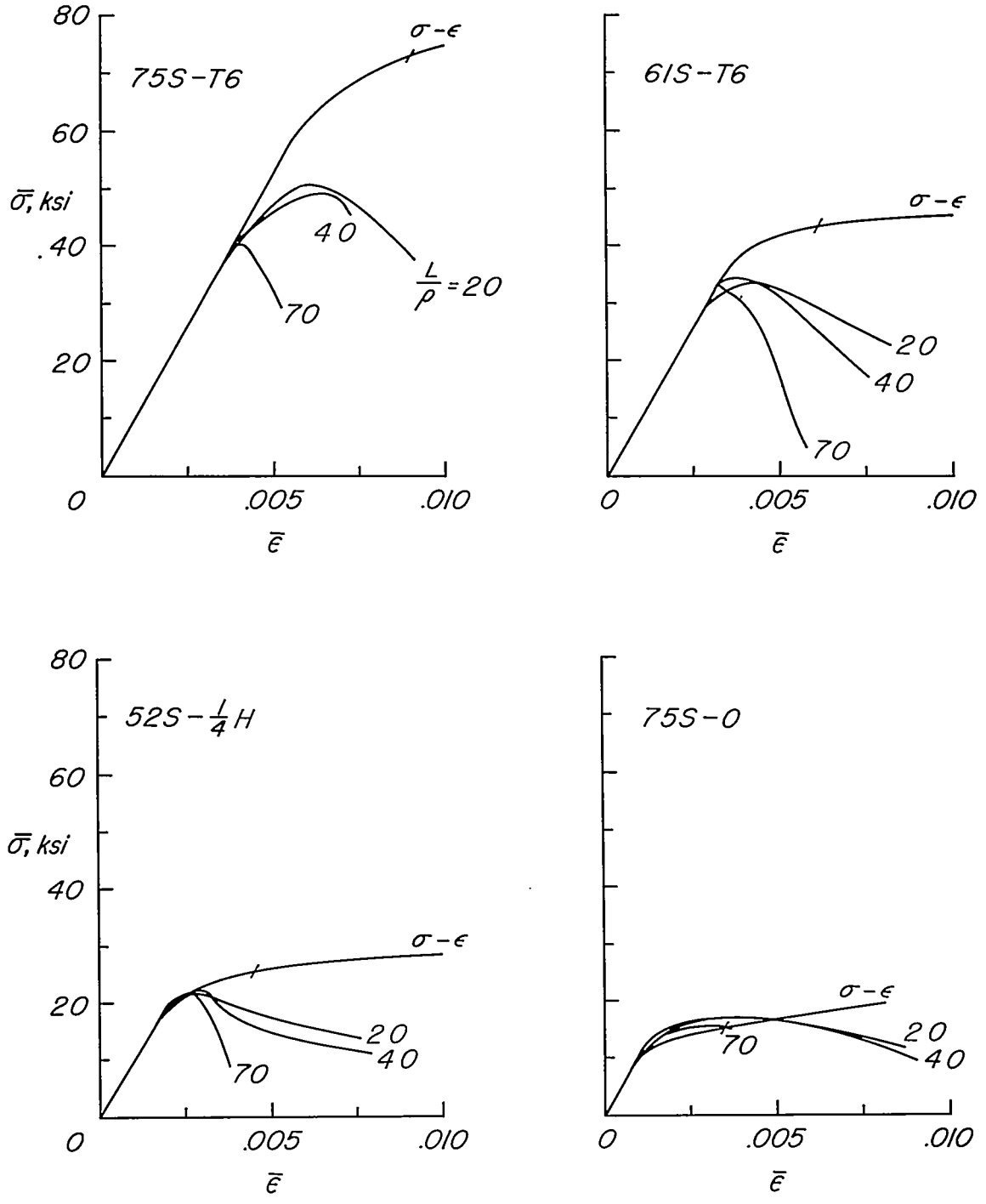

(b) $\frac{t_w}{t_s} = 1.00$; $\frac{b_w}{t_w} = 18.75$; $\frac{b_s}{t_s} = 37.5$.

Figure 4. – Continued.

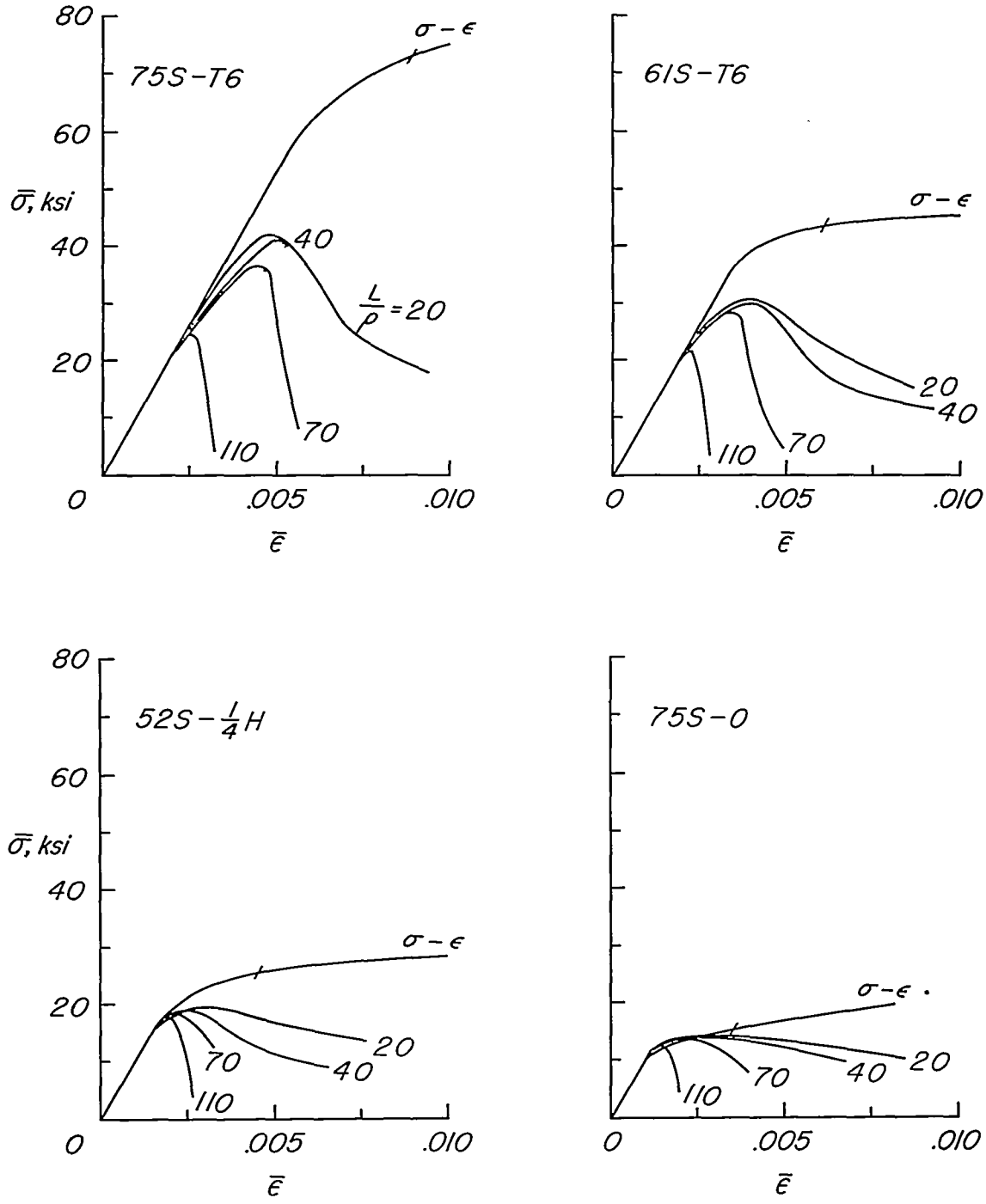

(c) $\frac{t_w}{t_s}=1.00$; $\frac{b_w}{t_w}=25$; $\frac{b_s}{t_s}=50$.

Figure 4. – Continued.

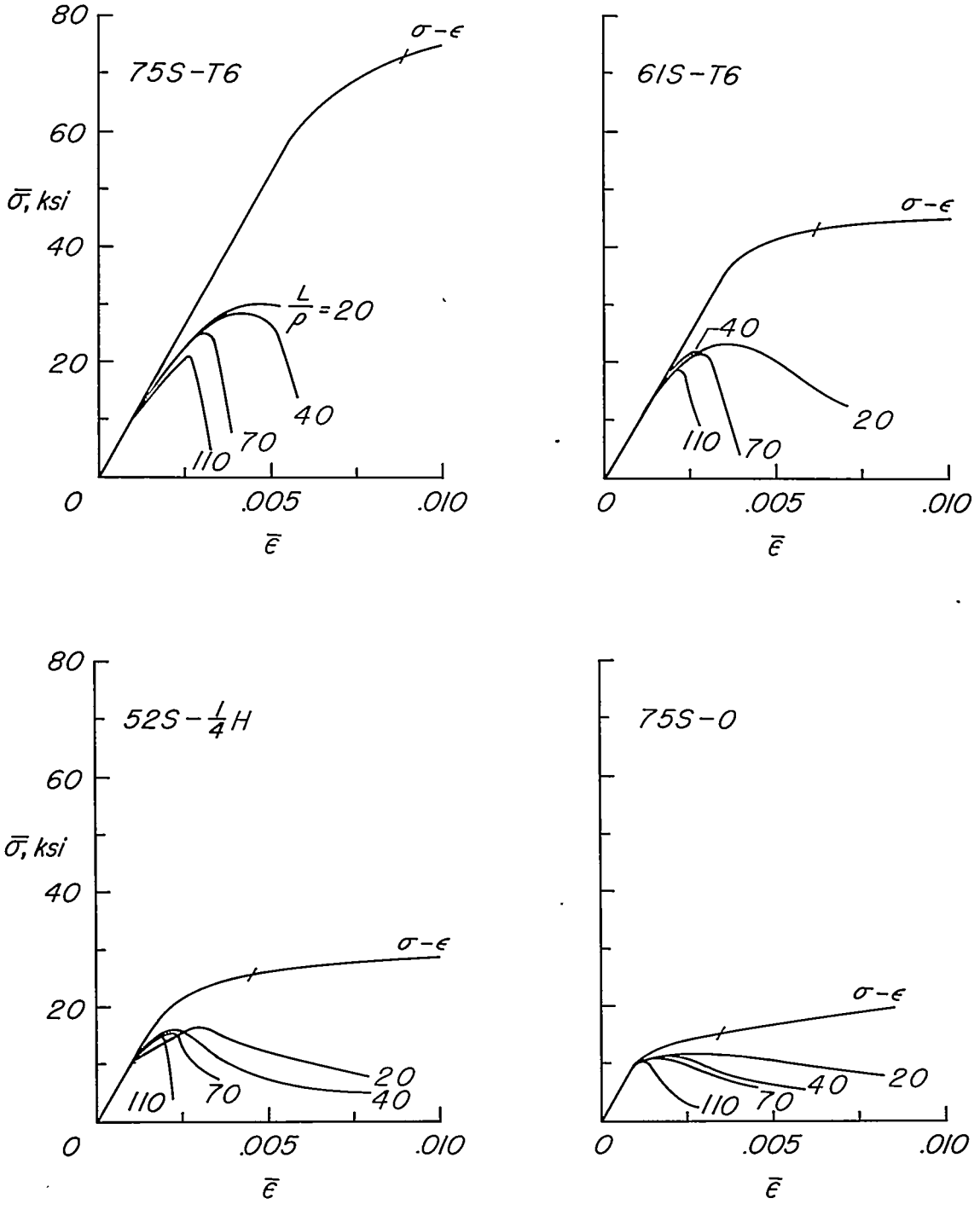

(d) $\frac{t_w}{t_s} = 1.00$; $\frac{b_w}{t_w} = 37.5$; $\frac{b_s}{t_s} = 75.$

Figure 4. – Continued.

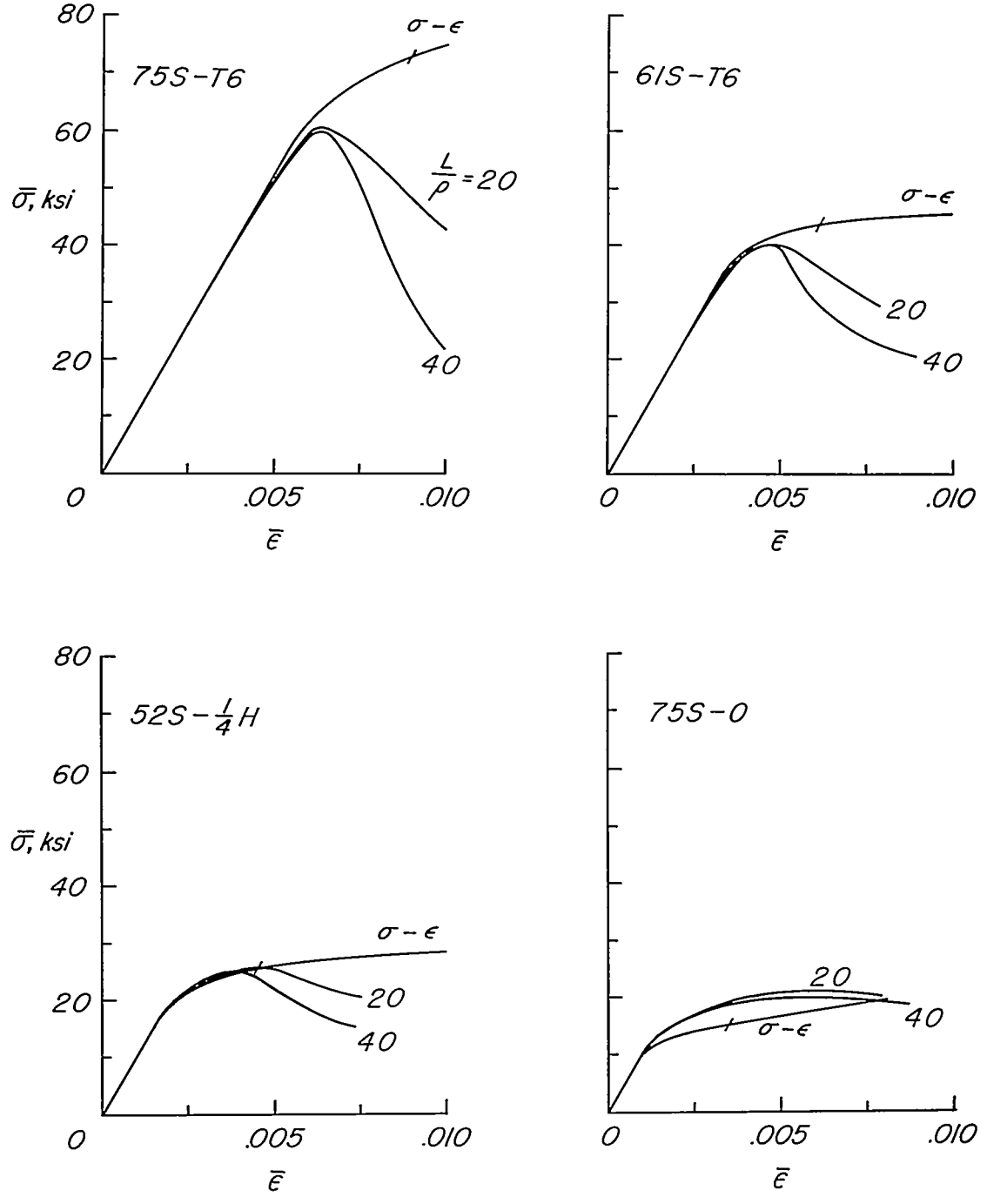

(e) $\frac{t_w}{t_s} = 1.00$; $\frac{b_w}{t_w} = 12.5$; $\frac{b_s}{t_s} = 25.$

Figure 4. — Continued.

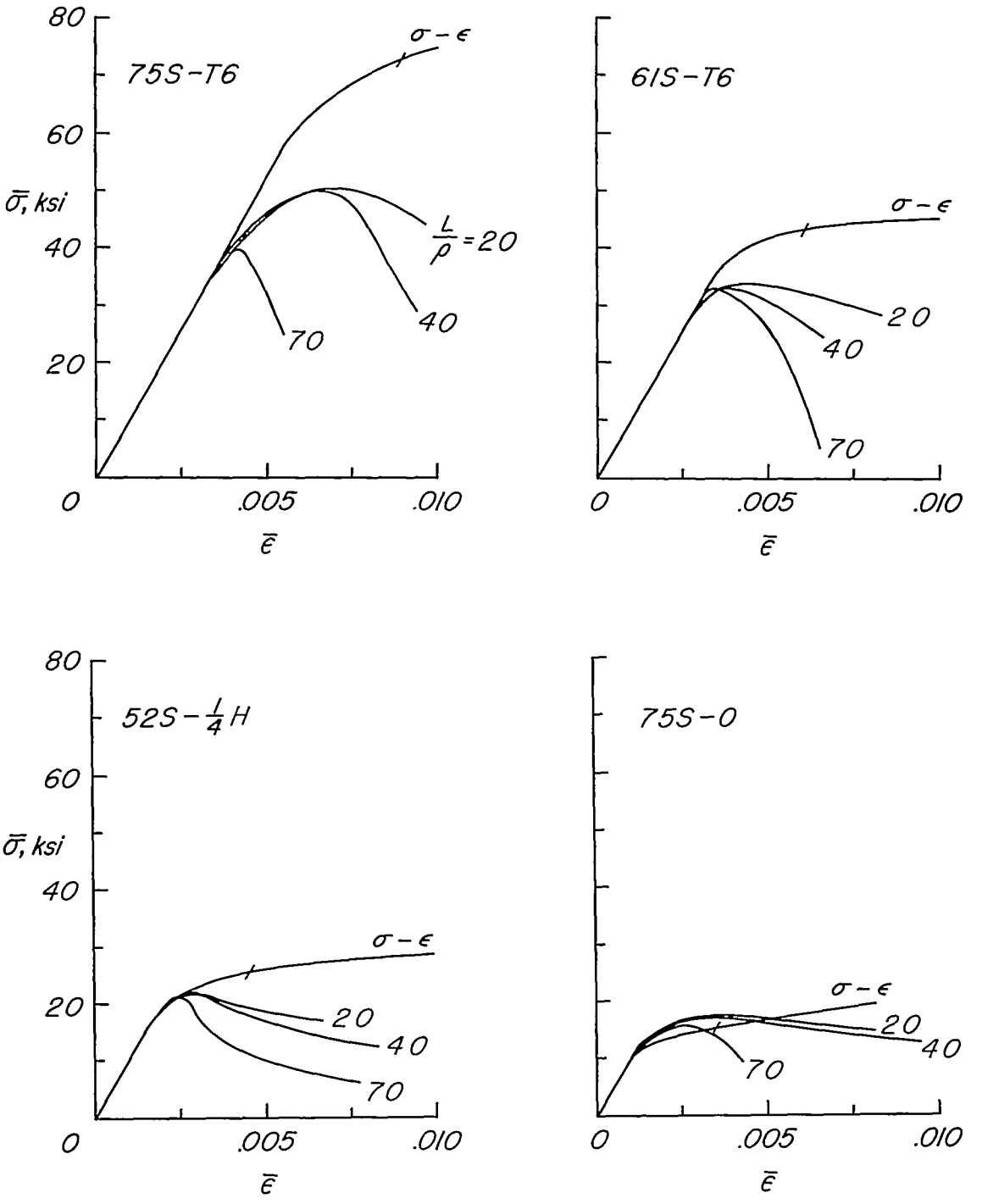

(f) $\frac{t_W}{t_S}=1.00$; $\frac{b_W}{t_W}=12.5$; $\frac{b_S}{t_S}=37.5$.

Figure 4. – Continued.

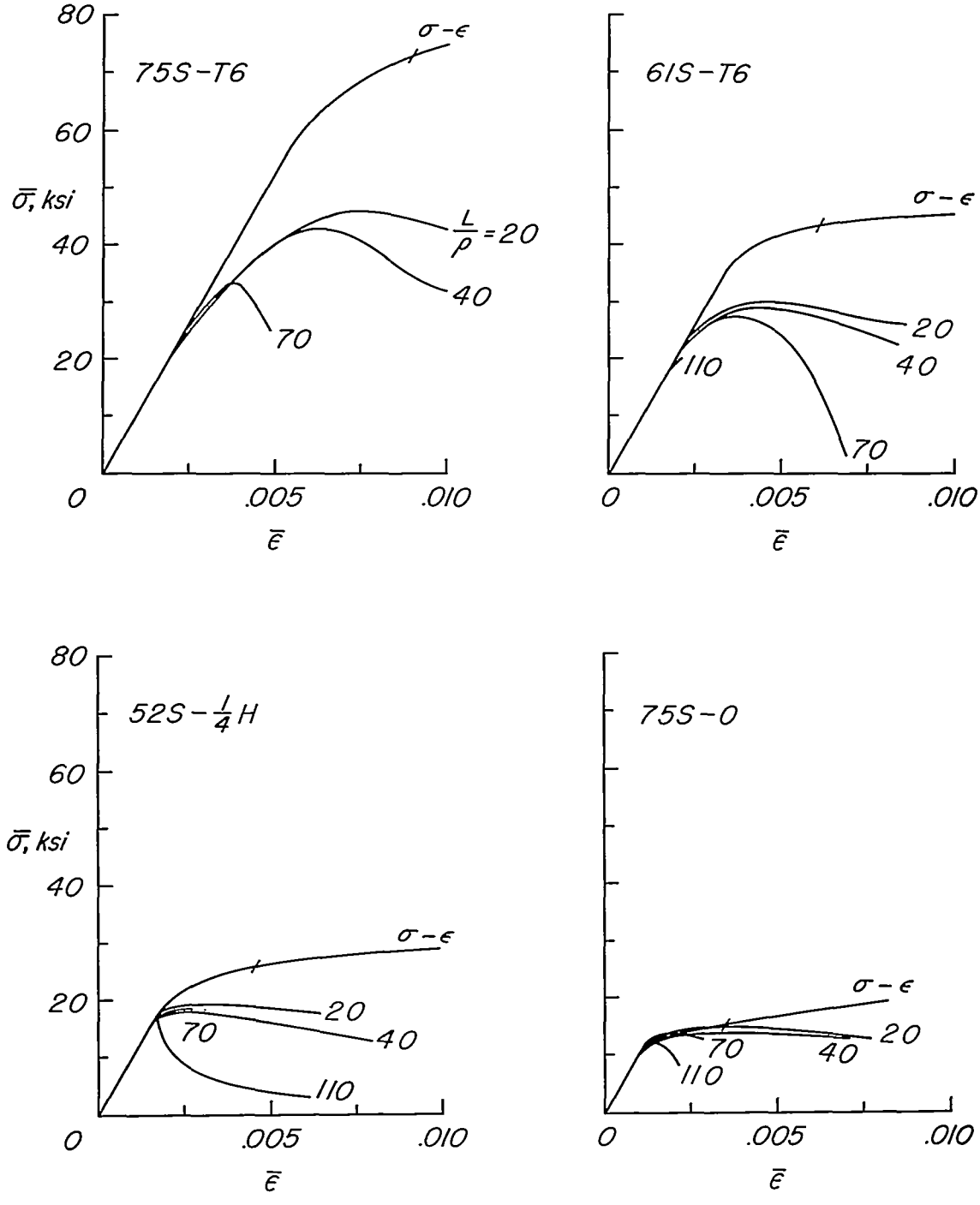

(g) $\frac{t_w}{t_s} = 1.00$; $\frac{b_w}{t_w} = 12.5$; $\frac{b_s}{t_s} = 50.$

Figure 4. – Continued.

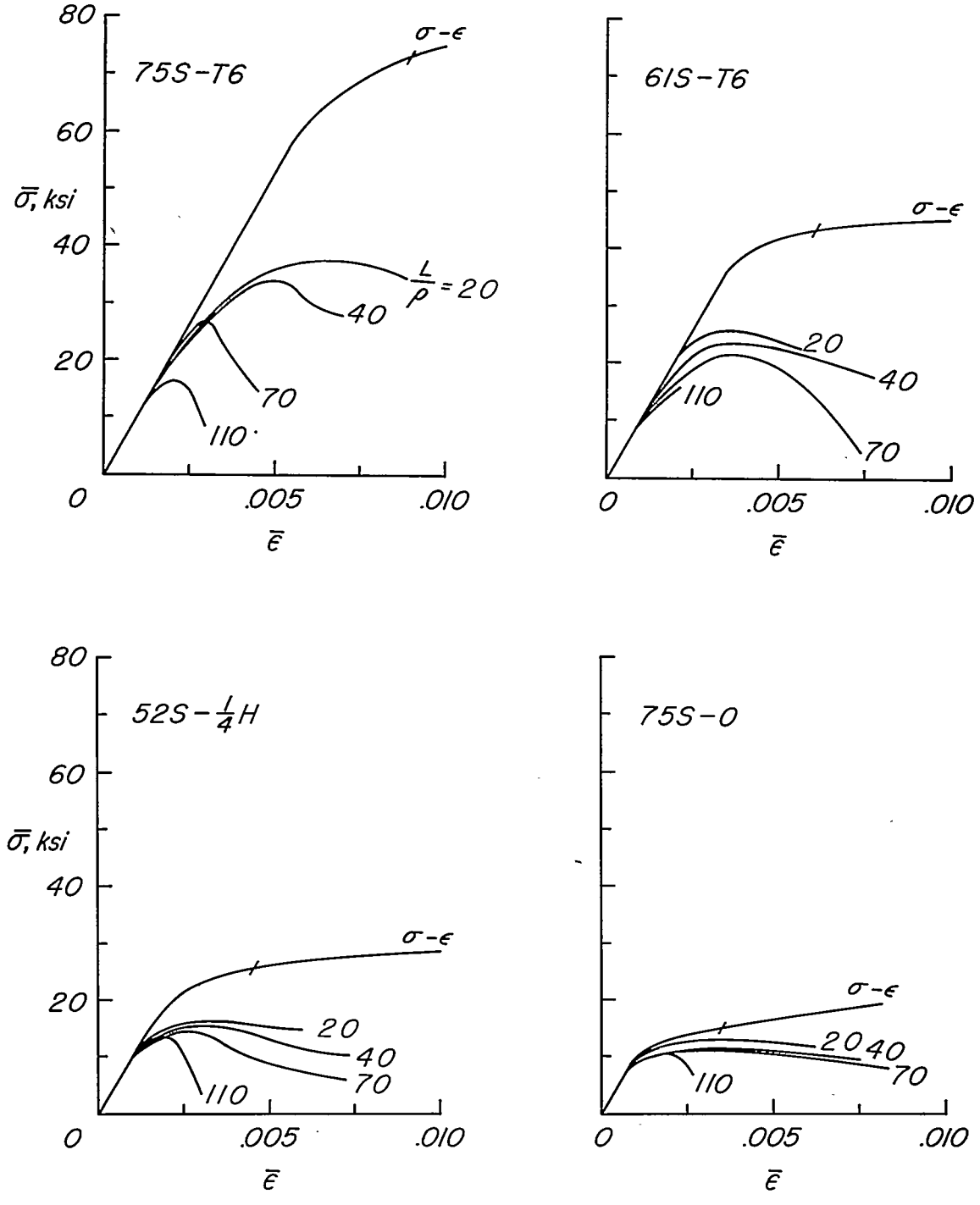

(h) $\frac{t_W}{t_S} = 1.00$; $\frac{b_W}{t_W} = 12.5$; $\frac{b_S}{t_S} = 75.$

Figure 4. – Concluded.

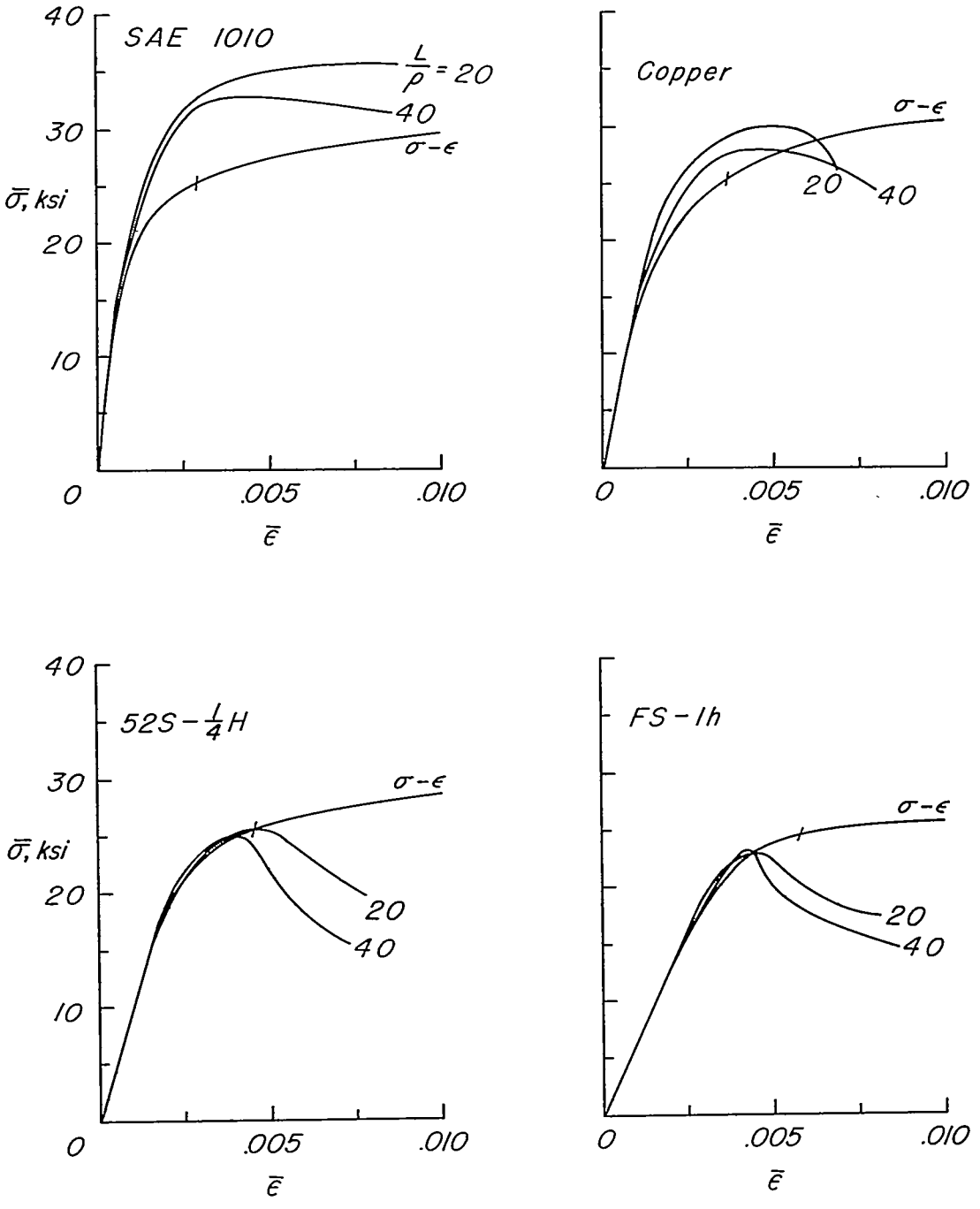

(a) $\frac{t_w}{t_s} = 1.00$; $\frac{b_w}{t_w} = 12.5$; $\frac{b_s}{t_s} = 25.$

Figure 5. – Curves of average stress against unit shortening for phase II panels.

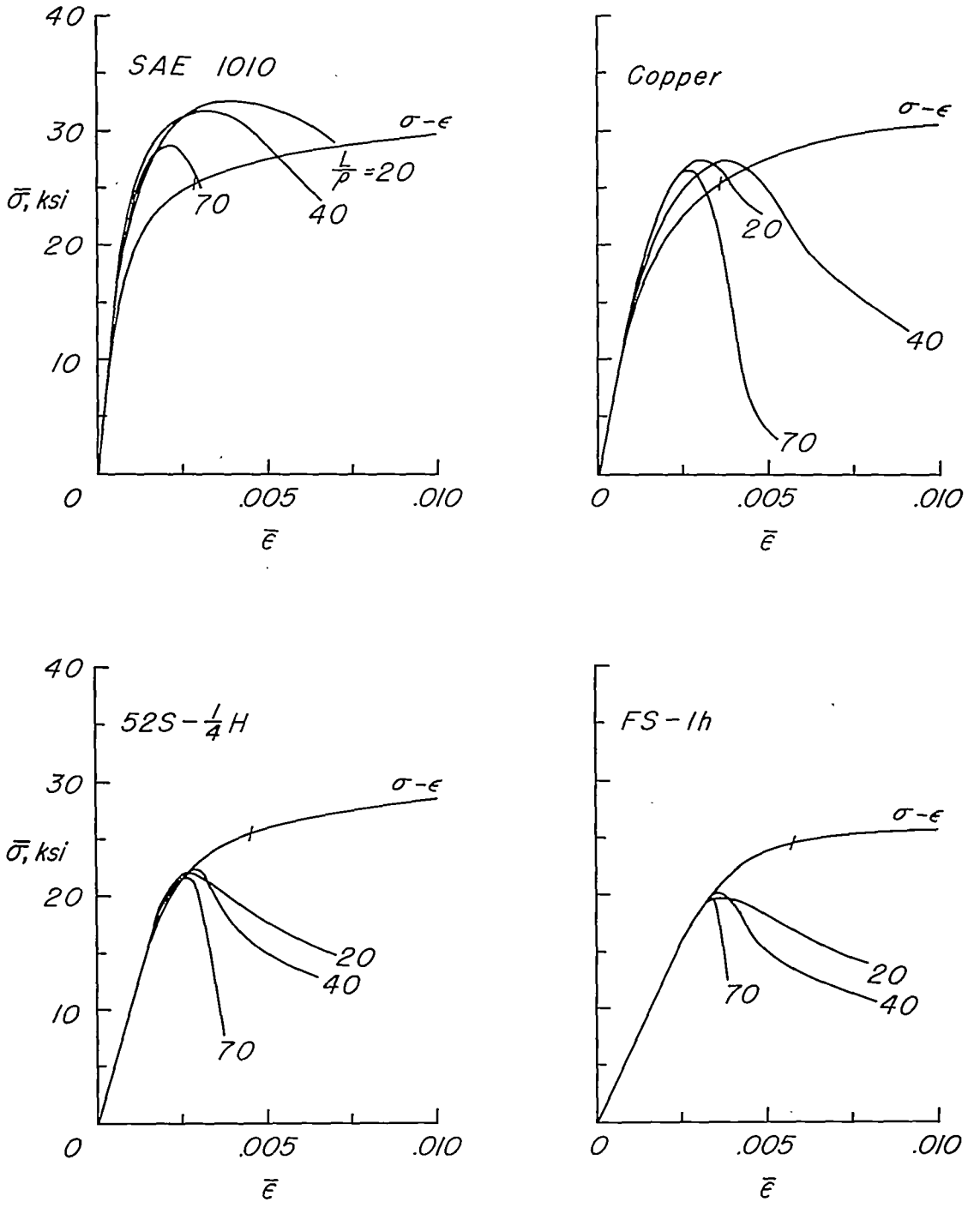

(b) $\frac{t_w}{t_s} = 1.00$; $\frac{b_w}{t_w} = 18.75$; $\frac{b_s}{t_s} = 37.5$.

Figure 5. – Continued.

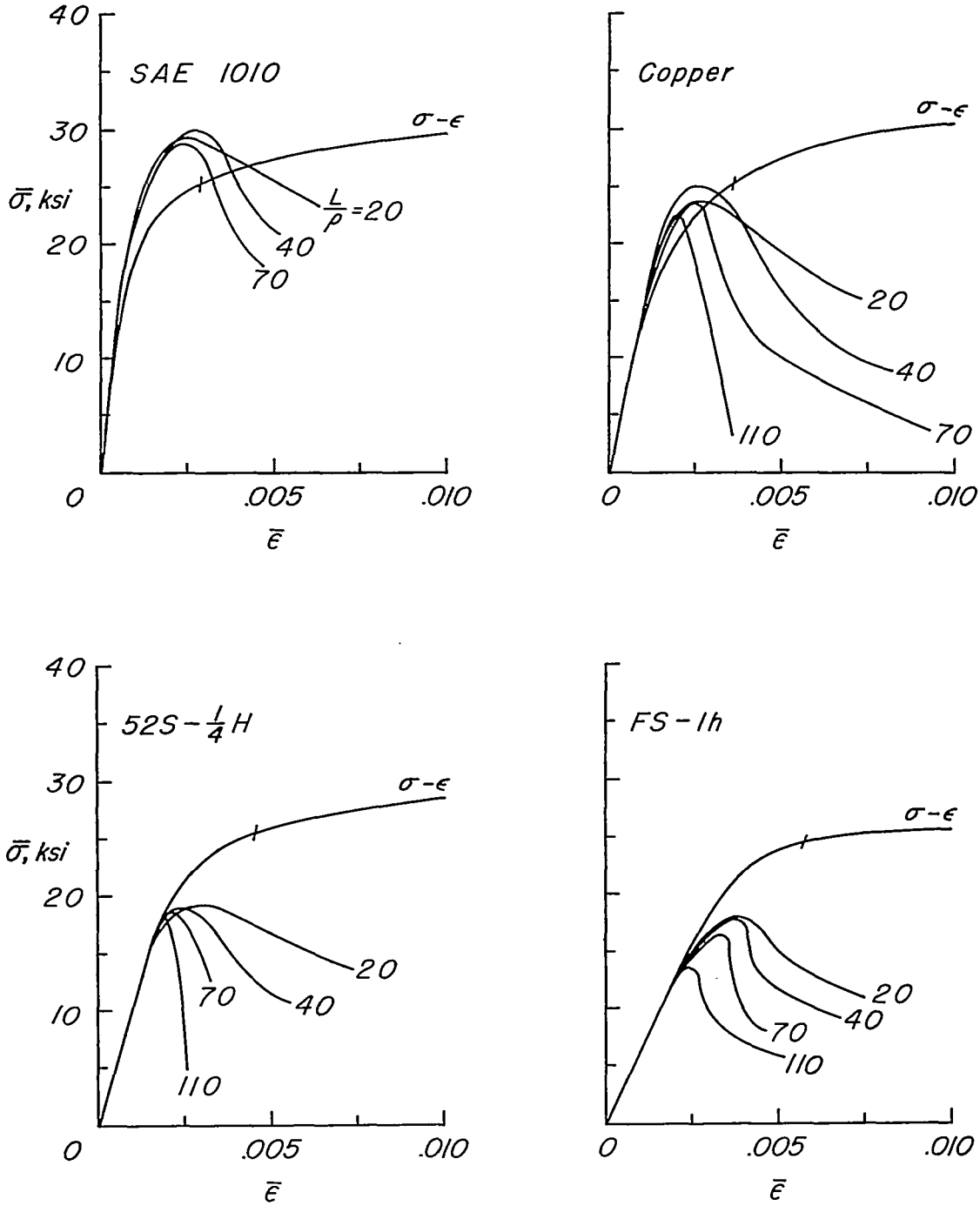

(c) $\frac{t_w}{t_s}=1.00; \frac{b_w}{t_w}=25; \frac{b_s}{t_s}=50.$

Figure 5. – Continued.

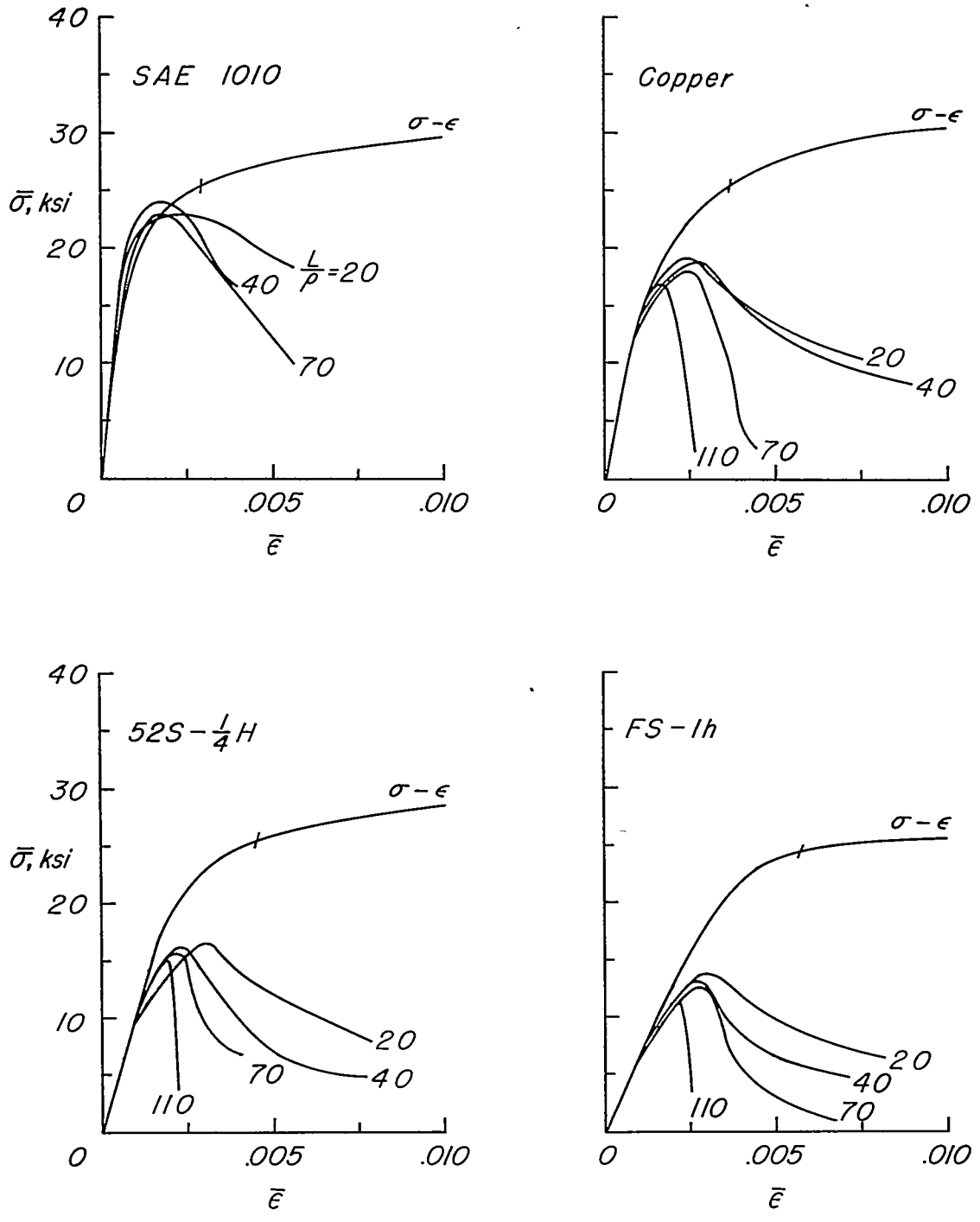

(d) $\frac{t_w}{t_s} = 1.00; \frac{b_w}{t_w} = 37.5; \frac{b_s}{t_s} = 75.$

Figure 5. – Continued.

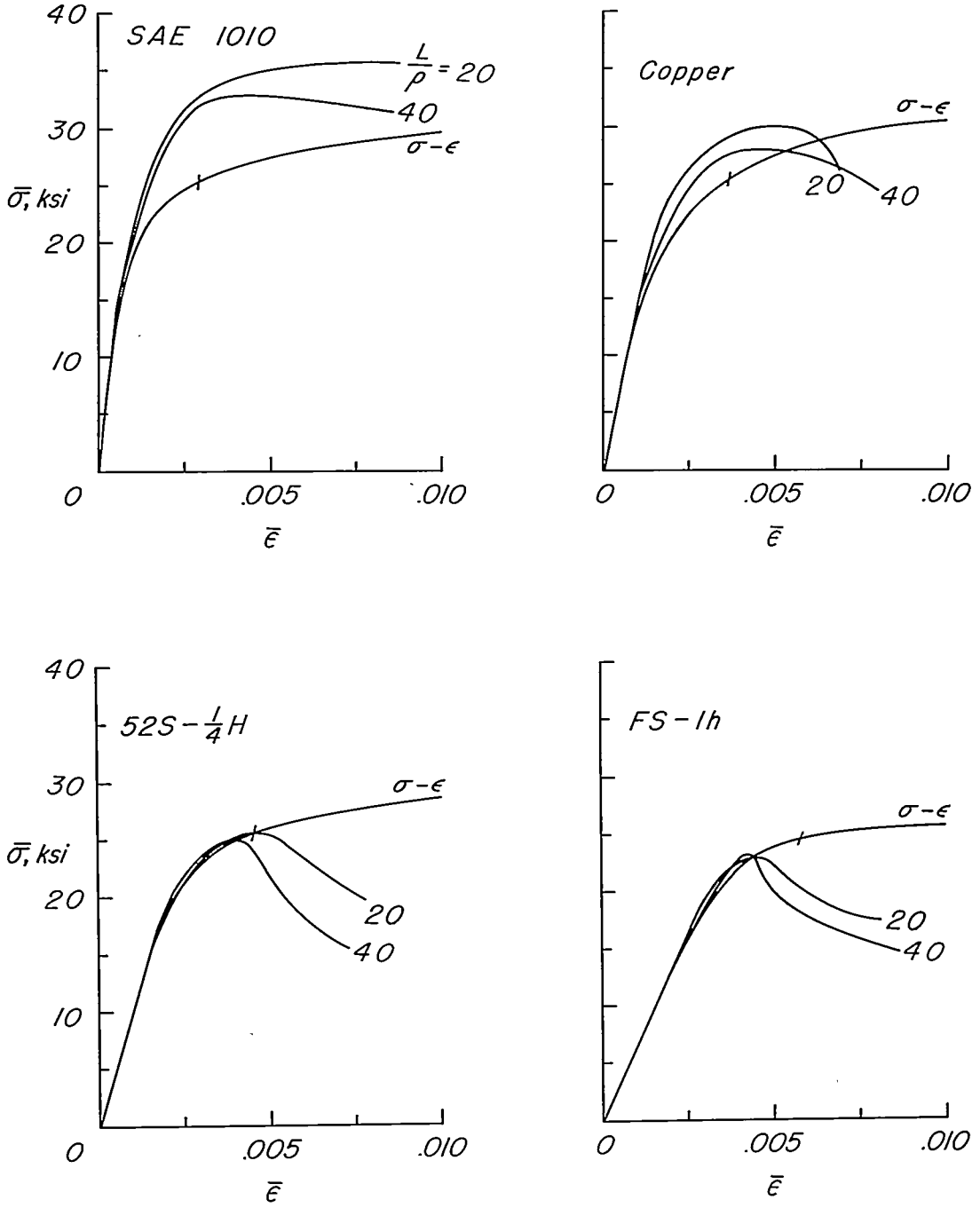

(e) $\frac{t_W}{t_S}$ = 1.00; $\frac{b_W}{t_W}$ = 12.5; $\frac{b_S}{t_S}$ = 25.

Figure 5. – Continued.

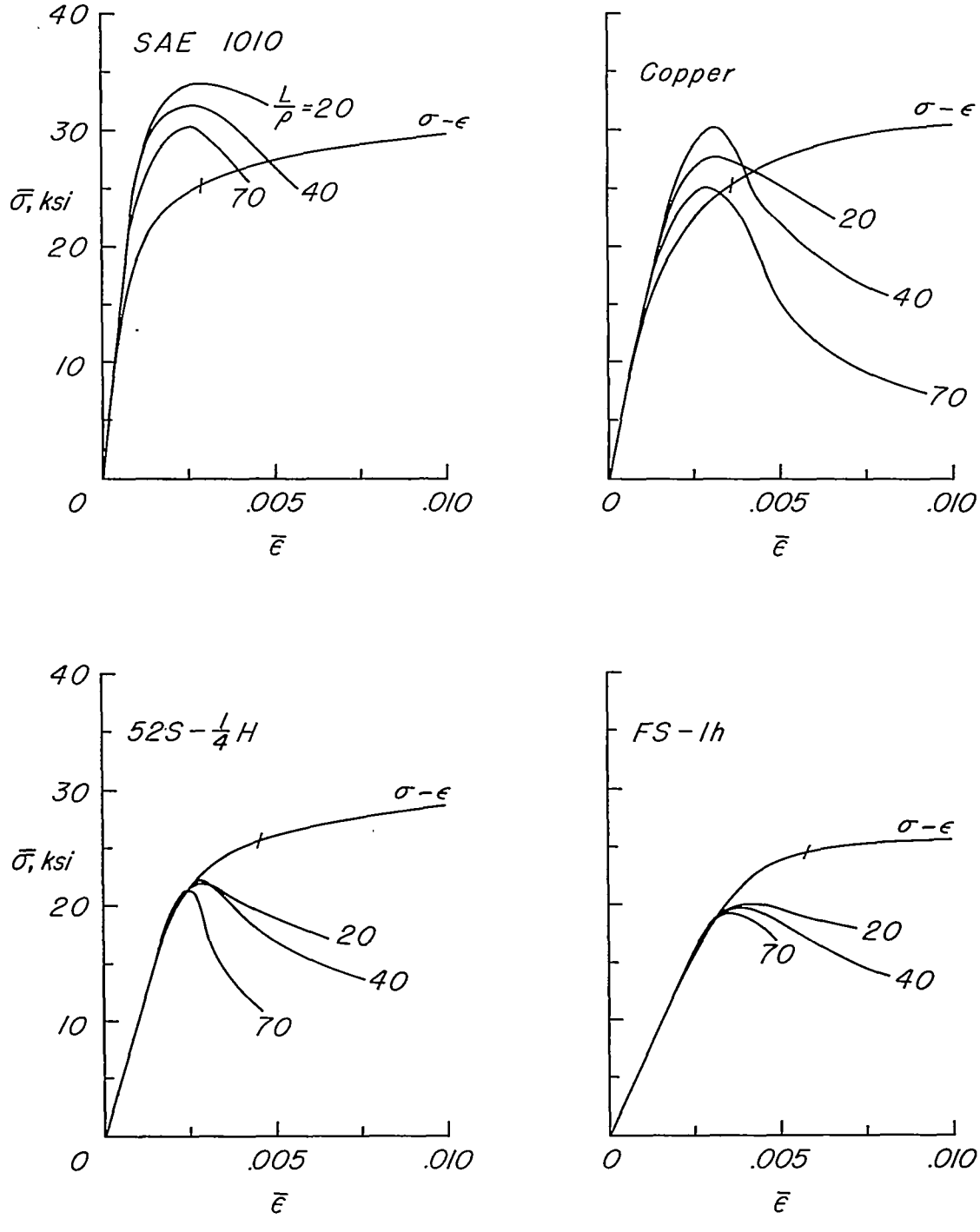

(f) $\frac{t_w}{t_s} = 1.00; \frac{b_w}{t_w} = 12.5; \frac{b_s}{t_s} = 37.5.$

Figure 5. – Continued.

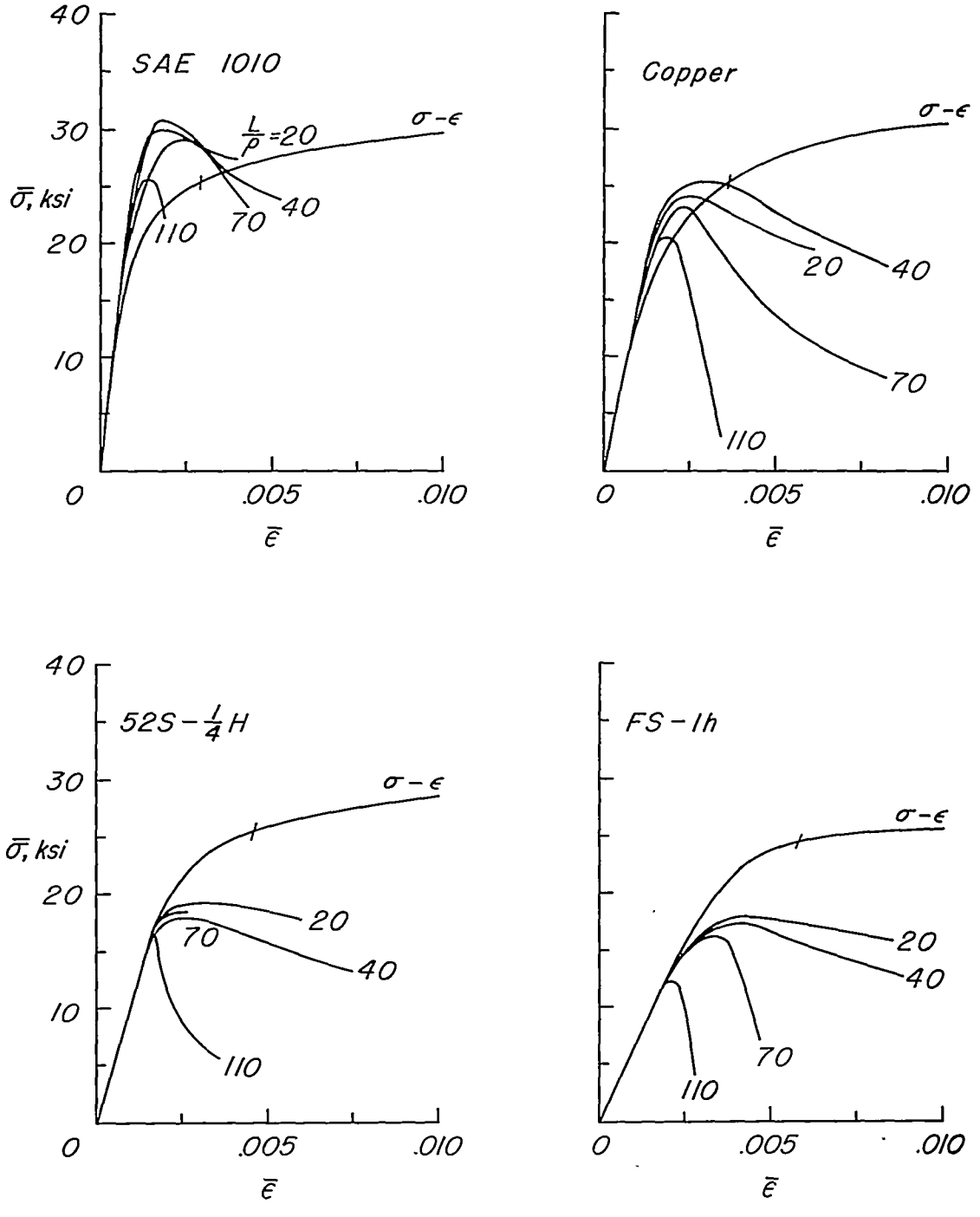

(g) $\frac{t_w}{t_s} = 1.00; \frac{b_w}{t_w} = 12.5; \frac{b_s}{t_s} = 50.$

Figure 5. – Continued.

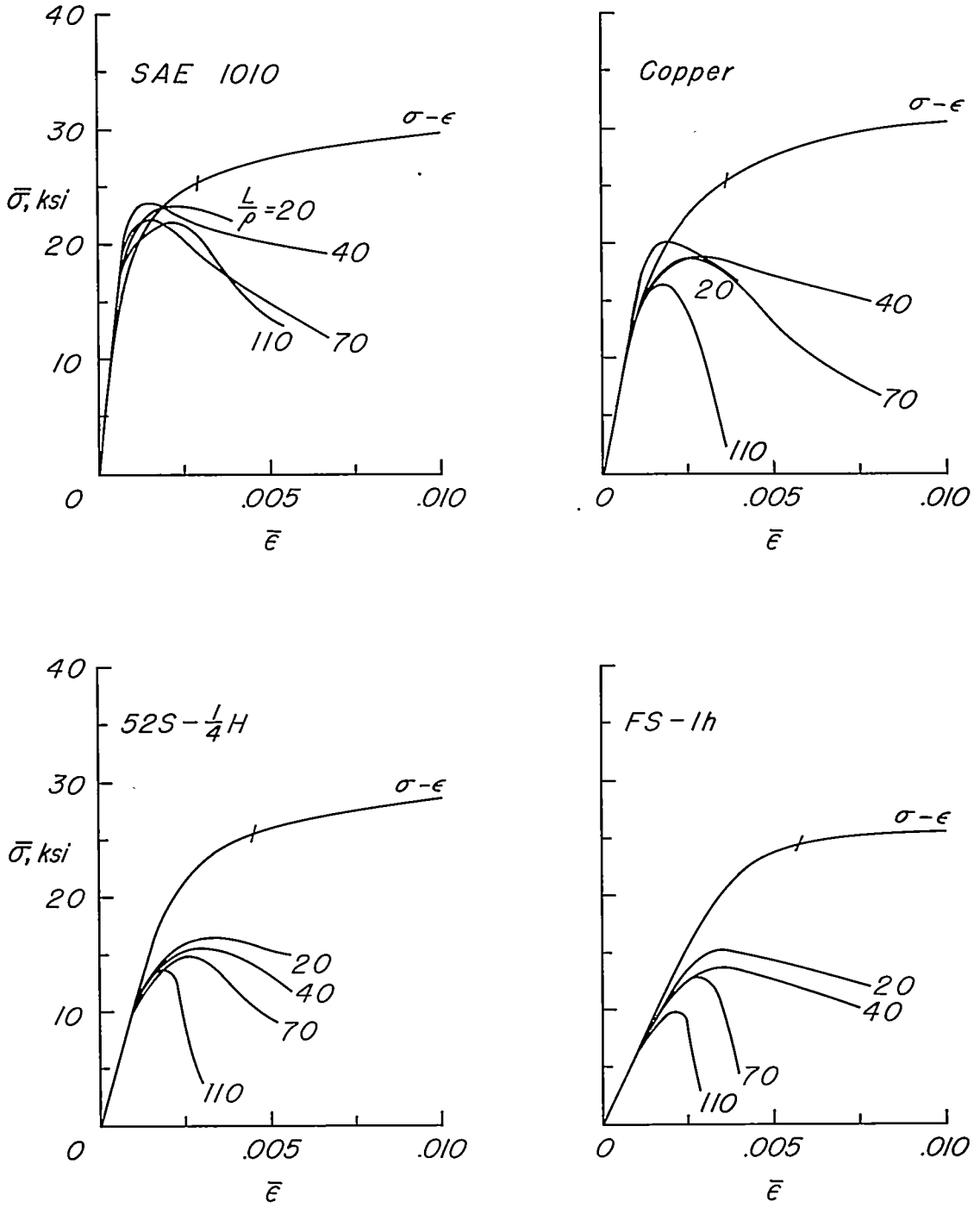

(h) $\frac{t_W}{t_S} = 1.00$; $\frac{b_W}{t_W} = 12.5$; $\frac{b_S}{t_S} = 75.$

Figure 5. – Concluded.

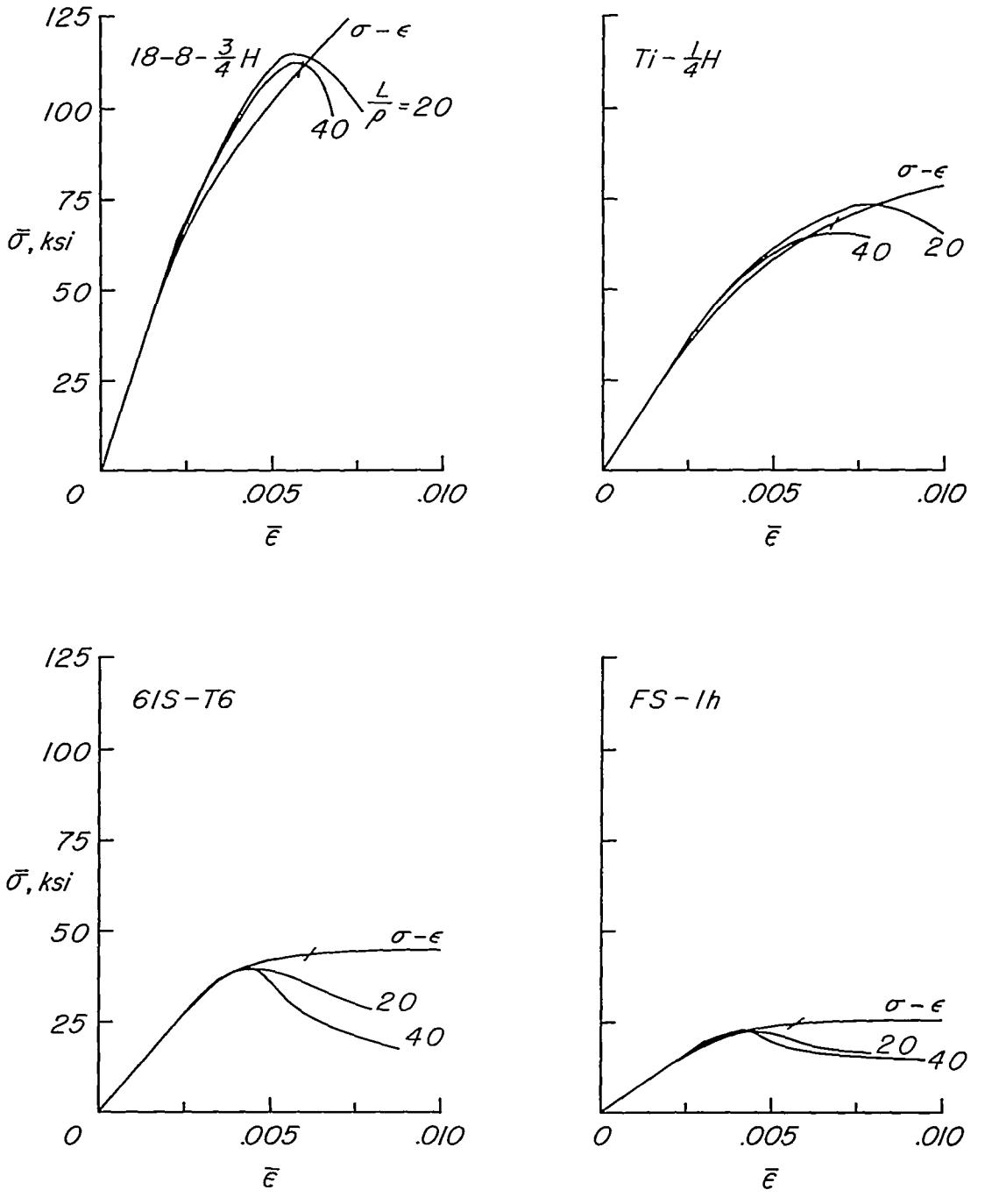

(a) $\frac{t_W}{t_S}=1.00$; $\frac{b_W}{t_W}=12.5$; $\frac{b_S}{t_S}=25.$

Figure 6. — Curves of average stress against unit shortening for phase III panels.

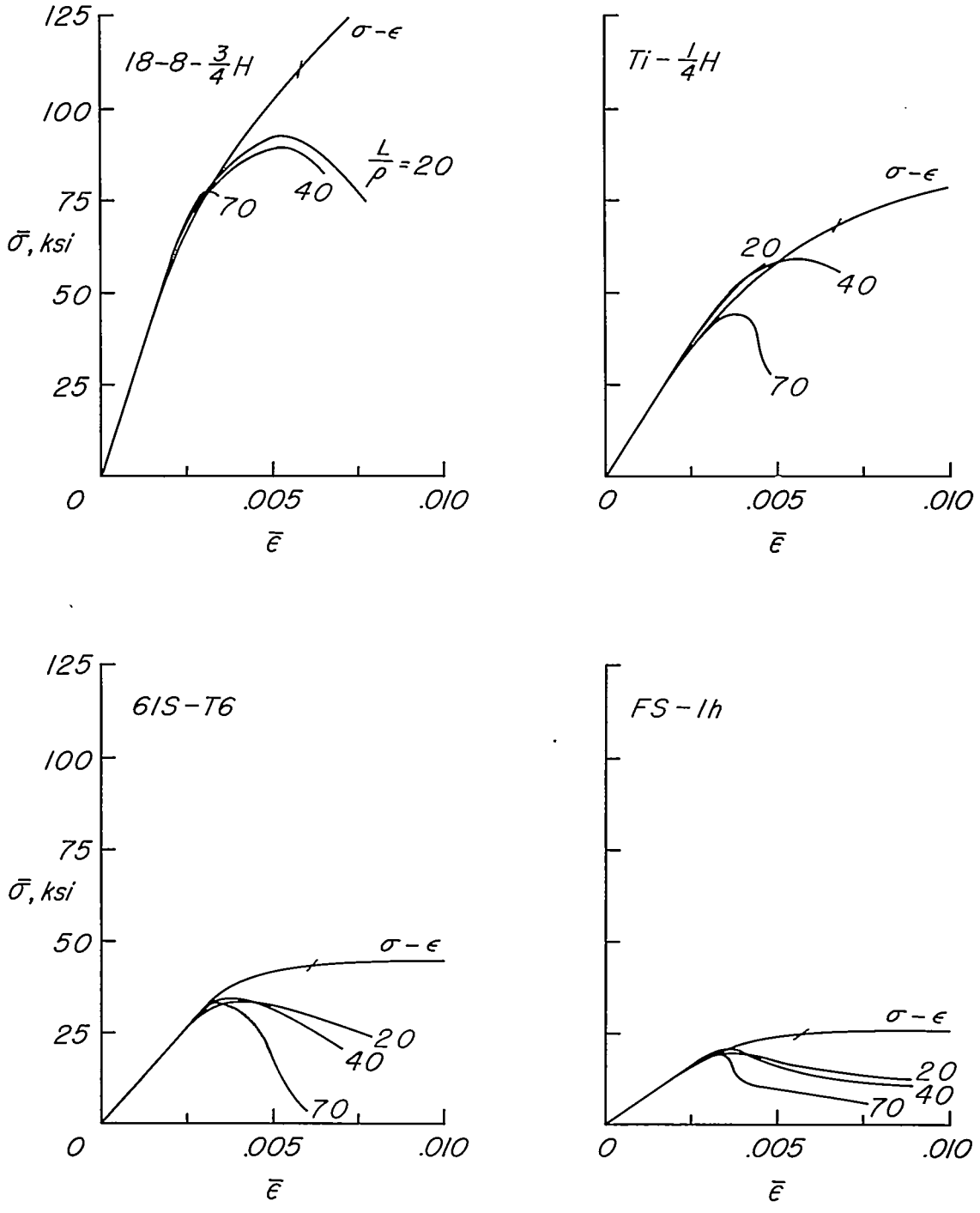

(b) $\frac{t_w}{t_s} = 1.00$; $\frac{b_w}{t_w} = 18.75$; $\frac{b_s}{t_s} = 37.5$.

Figure 6. - Continued.

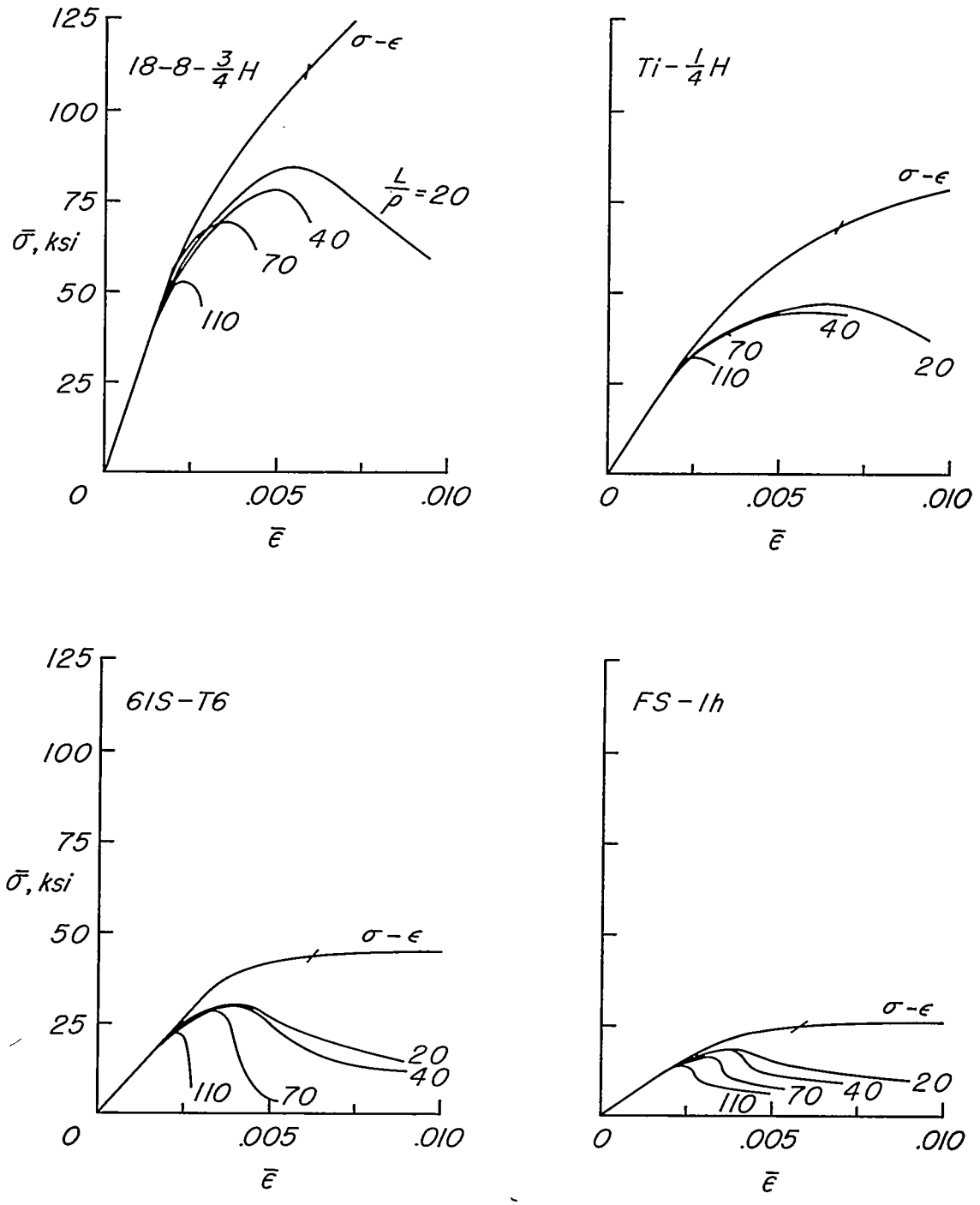

(c) $\frac{t_w}{t_s}=1.00$; $\frac{b_w}{t_w}=25$; $\frac{b_s}{t_s}=50$.

Figure 6. – Continued.

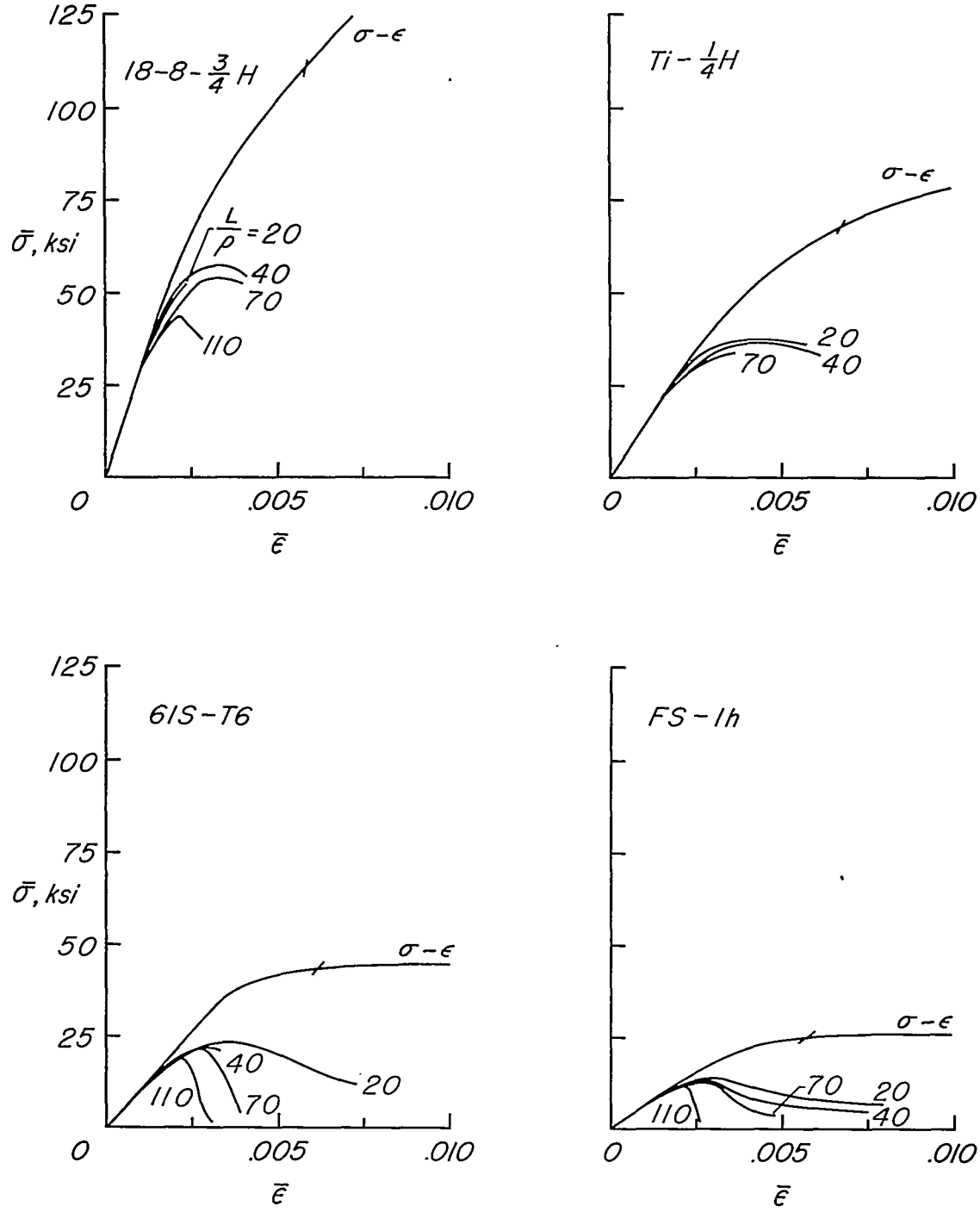

(d) $\frac{t_w}{t_s} = 1.00; \frac{b_w}{t_w} = 37.5; \frac{b_s}{t_s} = 75.$

Figure 6. – Continued.

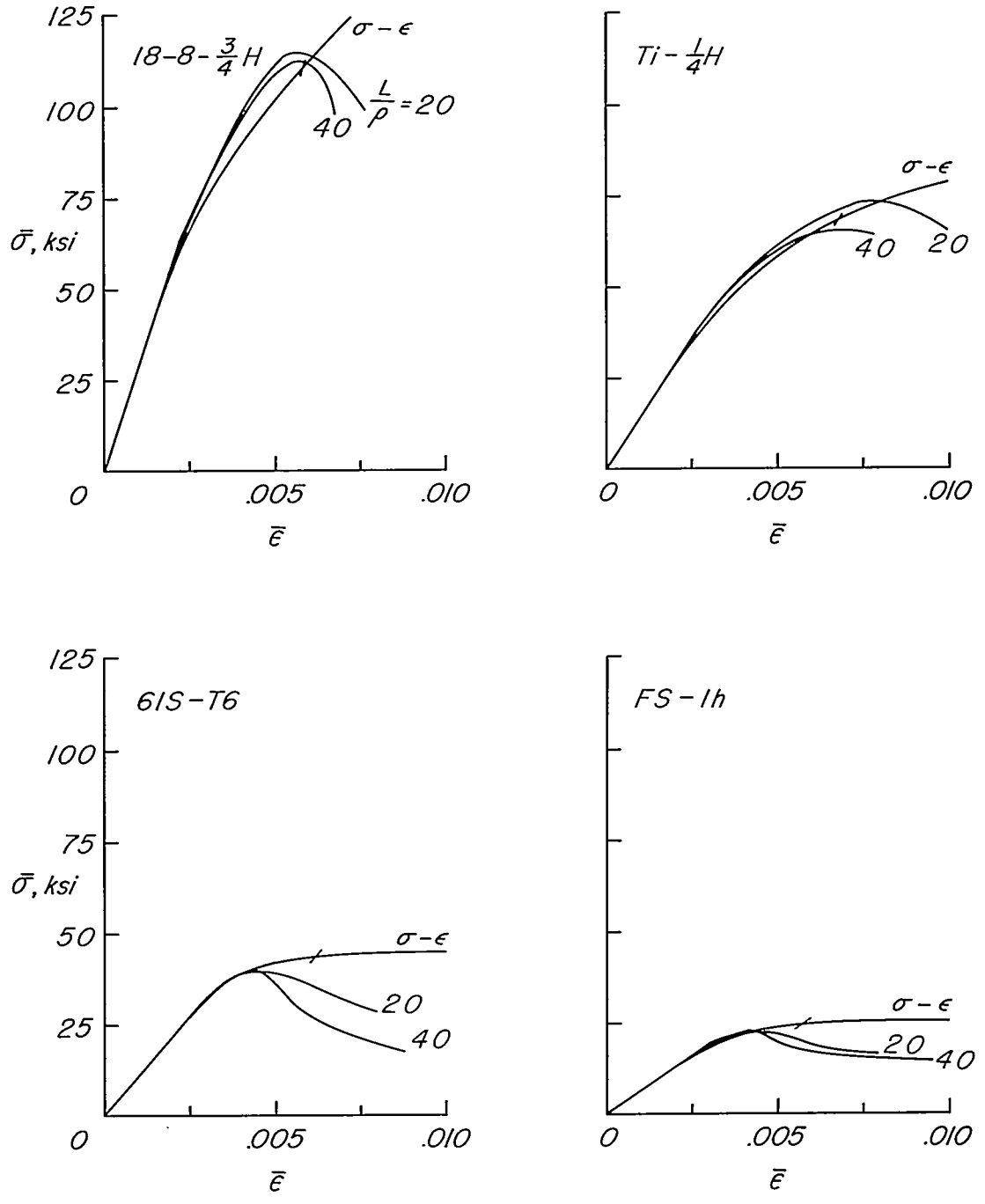

(e) $\frac{t_W}{t_S}$ = 1.00; $\frac{b_W}{t_W}$ = 12.5; $\frac{b_S}{t_S}$ = 25.

Figure 6. – Continued.

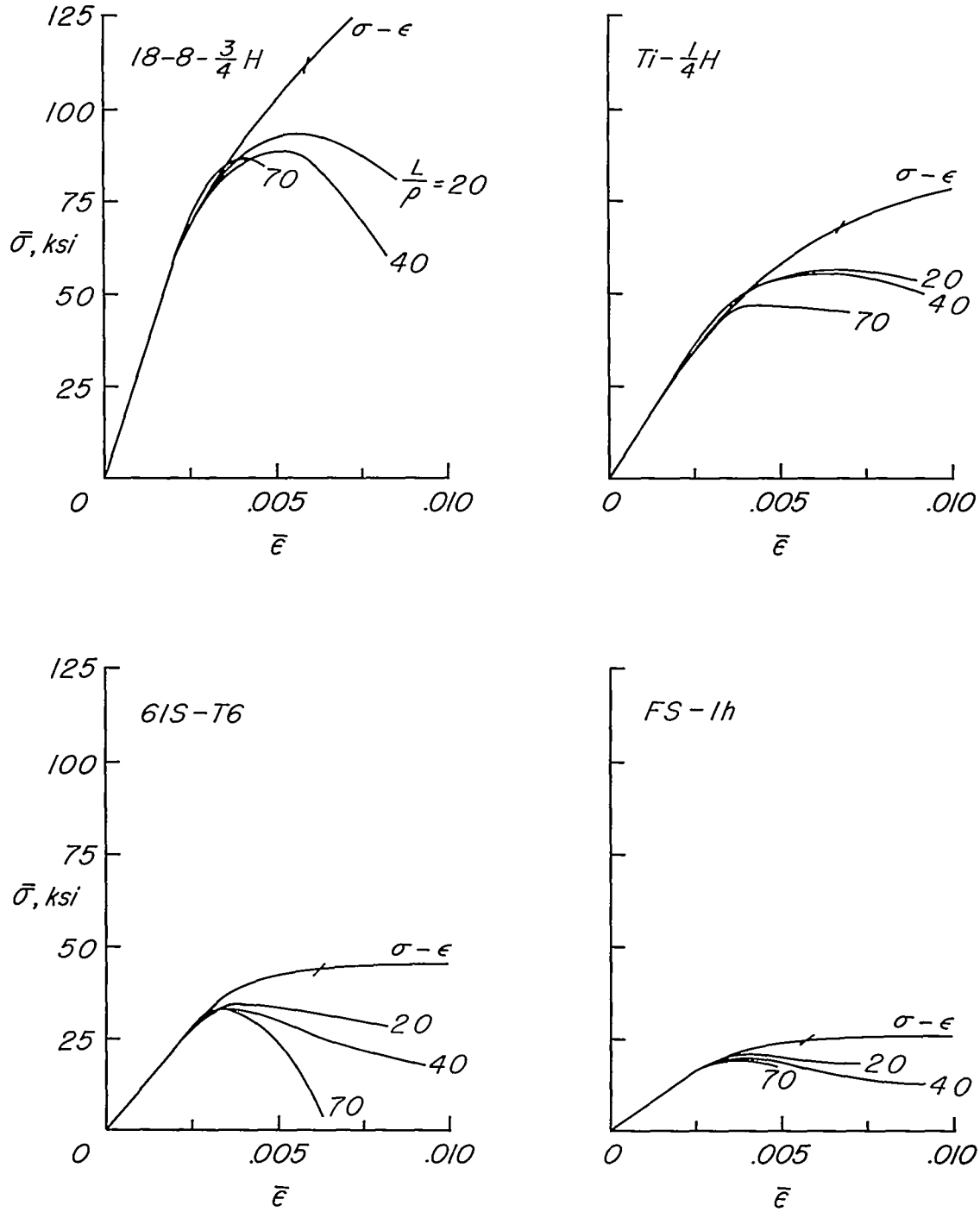

(f) $\frac{t_w}{t_s} = 1.00; \frac{b_w}{t_w} = 12.5; \frac{b_s}{t_s} = 37.5.$

Figure 6. – Continued.

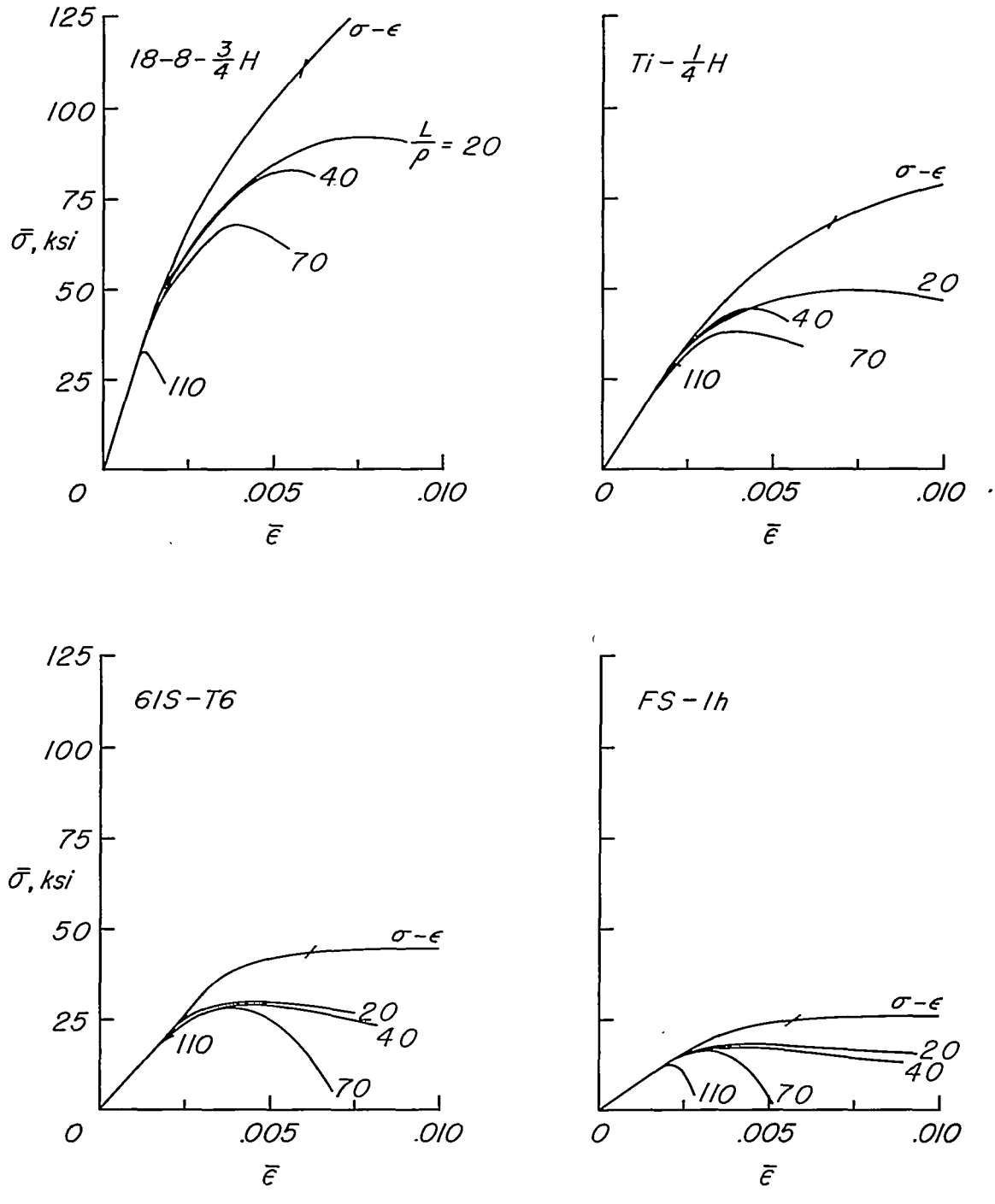

(g) $\frac{t_W}{t_S} = 1.00$; $\frac{b_W}{t_W} = 12.5$; $\frac{b_S}{t_S} = 50$.

Figure 6. – Continued.

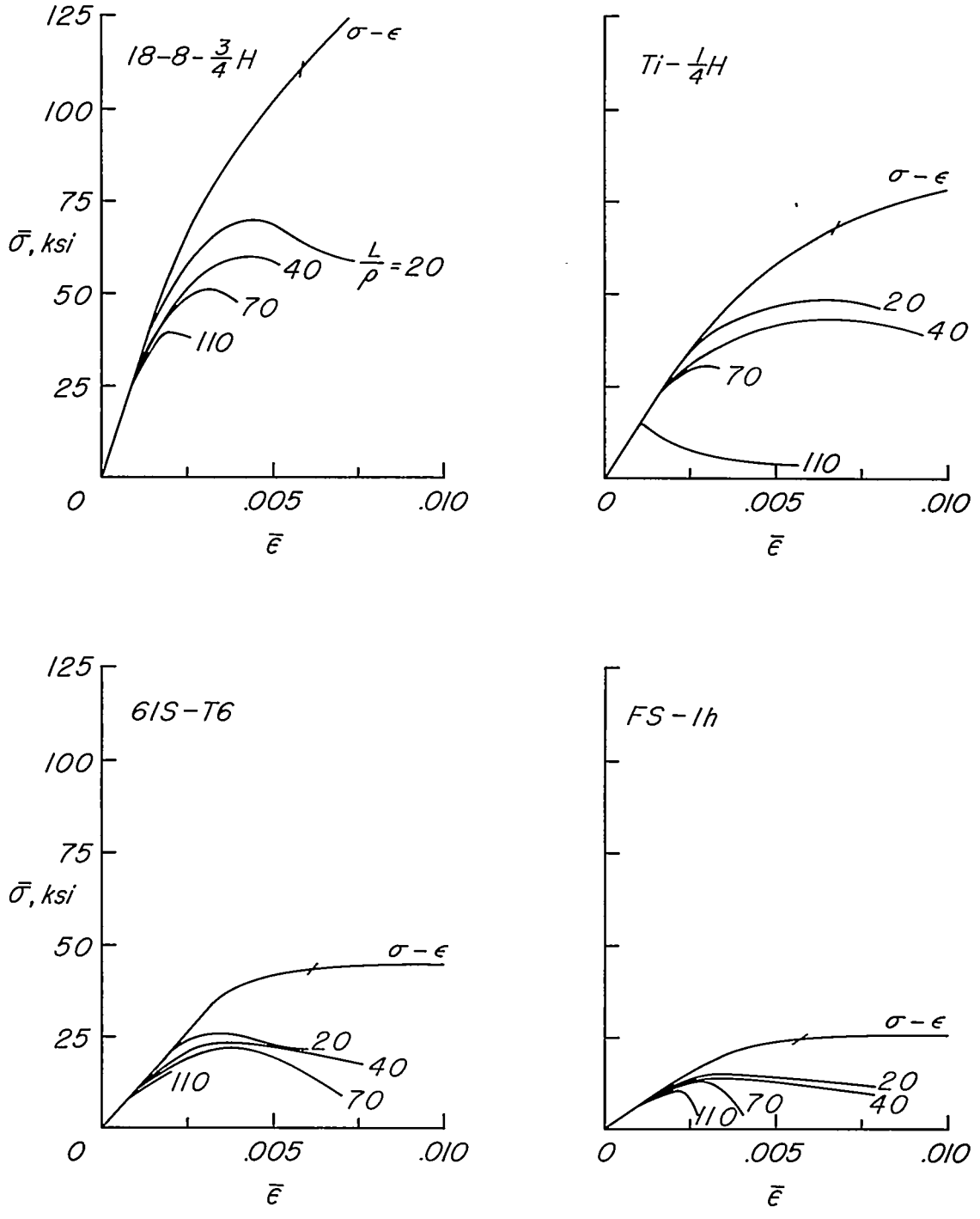

(h) $\frac{t_W}{t_S} = 1.00$; $\frac{b_W}{t_W} = 12.5$; $\frac{b_S}{t_S} = 75$.

Figure 6. - Concluded.

NACA-Langley - 1-20-54 - 1000